University of Stavanger

Faculty of Science and Technology

MASTER'S THESIS

Study program/Specialization: Industrial Economics and Technology Management w/ specialization in Project Management	Spring semester, 2021 Open / Restricted access
Writer: Ajhanth Yogachandran	Ajhanth ………………………………………………… (Writer's signature)
Faculty supervisor: Reidar Brumer Bratvold and Aojie Hong, University of Stavanger External supervisor(s):	
Thesis title: An analysis of gas production forecasts on the NCS	
Credits (ECTS): 30	
Key words: Gas NPD Bias PDO Probability Delay NCS Unbiased forecast	Pages: ………58………… + enclosure: …14(62-75)… Stavanger, 05/06/2021 Date/year

An analysis of gas production forecasts on the NCS

Ajhanth Yogachandran

July 6, 2021

Version: Master's Thesis

Abstract

Thesis assess operators ability to deliver accumulated gas forecasts for 40 fields on the Norwegian continental shelf (NCS) that received Plan for Plan for Development and Operations (PDO) approval in the years 2000 to 2020. The analysis is conducted both with and without including schedule delays. The results indicate that operators forecasts are heavily influenced by optimism and overconfidence bias resulting in significantly lower production than forecasted and that was the basis for the investment decisions. However, this study shows that the forecasts are particularly poor in the early part of field life and improves toward the end of field lives.

Acknowledgement

This thesis helps me to complete my graduation in the Industrial Economics and Technology Management master´s programme at the University of Stavanger. First and foremost, I would like to thank my supervisors, professor Reidar Bratvold and professor Aojie Hong, who gave me the possibility to work with a quantitative thesis, which I was looking for. Since the start of my thesis writing, they have been a strong support for me with their concrete feedback. I have had difficult moments when working with this thesis, but luckily so, I received valuable suggestions and ideas to overcome the difficulties I have encountered. I owe the Norwegian petroleum Directorate for making the saleable forecasts feasible under a non-disclosure agreement, which enabled the study. Furthermore, I would like to thank, professor Erik Nesvold, who gave me more insights and clarity regarding the raw RNB dataset.

Secondly, I would like to thank my family and close relatives, who have supported me throughout this process of completing a master´s degree in Industrial Economics and Technology Management. I am glad that I can make them proud, and finally receive the title as a civil engineer.

Finally, I would like to thank the University of Stavanger and the Faculty of Science and Technology for giving me the opportunity to complete my master´s degree in Industrial Economics and Technology Management.

List of Figures

List of Tables

Abbreviations

F0Y First zero year

F1Y First one year

F2Y First two years

F3Y First three years

F4Y First four years

F5Y First five years

F6Y First six years

F8Y First eight years

F7Y First seven years

F9Y First nine years

F10Y First ten years

F11Y First eleven years

F12Y First twelve years

F13Y First thirteen years

F14Y First fourteen years

F15Y First fifteen years

F16Y First sixteen years

F17Y First seventeen years

F43Y First forty three years

F49Y First forty nine years

TVM Time value of Money

VoI Value of Information

NPD Norwegian Petroleum Directorate

FID final investment decision

PDO Plan for Development and Operations

NCS Norwegian continental shelf

PDFs probability density functions

CDFs cumulative-distribution functions

PDF probability density function

CDF cumulative-distribution function

MPE Ministry of Petroleum and Energy

RNB Revised National Budget

FXY First X years

podp pair of data points

U Unlimited

NPV Net present value

MG metalog

EV Expected value

IRR Internal rate of return

RCF Reference class forecasting

List of contents

1 Introduction

The discovery of oil and gas in the late 1960´s has had a tremendous influence in the Norwegian economy. Today the petroleum industry is seen as the most important source for income in Norway, and they are also a major supplier of both oil and gas to many countries worldwide.

Important decisions have to be made when considering development/redevelopment of fields on the NCS. Companies choose a decision criterion, usually the Net present value (NPV), and then make their decision based on that. Production forecasts are important because they are necessary inputs to develop the cash flow which, in turn, is used to calculate the NPV. As Bratvold et al. have discussed, the production forecasts are often related to revenues. The key decisions here are: (1) whether a field should be developed, and (2) if the answer to (1) is “yes”, how should the field be developed. Therefore, the forecast of production in this case is used as an input to calculate NPV. These key decisions do have a huge impact on saleable gas. Note that, words such as "forecasted" and "estimated" will from now on be used as synonyms.

When the operators deliver production forecasts for fields on the NCS, the forecasts deviate to some extent compared to the actual production. As a result of that, cost-and-time overruns occur, which could potentially change the entire scope when considering the development/redevelopment of fields. Although, the technology used in the petroleum industry is more robust and reliable today than in the beginning of the recovery, there is significant gap between the production forecast and the actual production. Being *bias* when making decisions, is more common rather than exception in the petroleum industry. This tendency influences the production forecasts, which again affects the saleable forecasts for gas.

The research done by Bratvold et al. for fields on the NCS shows that only 31% of the actual production lies within the forecasted 80% range for the first 4 years after production start for oil. A well calibrated production forecast is unbiased if 50% and 10% of actual production are lower than P50 and P10, respectively. Furthermore, the research shows that the actual productions were 84% and 59% for P50 and P10, respectively. Using the work done by Bratvold et al. (2020) as a basis, we are going to compare the forecasts for saleable gas with actual saleable gas, both with and without schedule delay, and see how the results effect the petroleum industry.

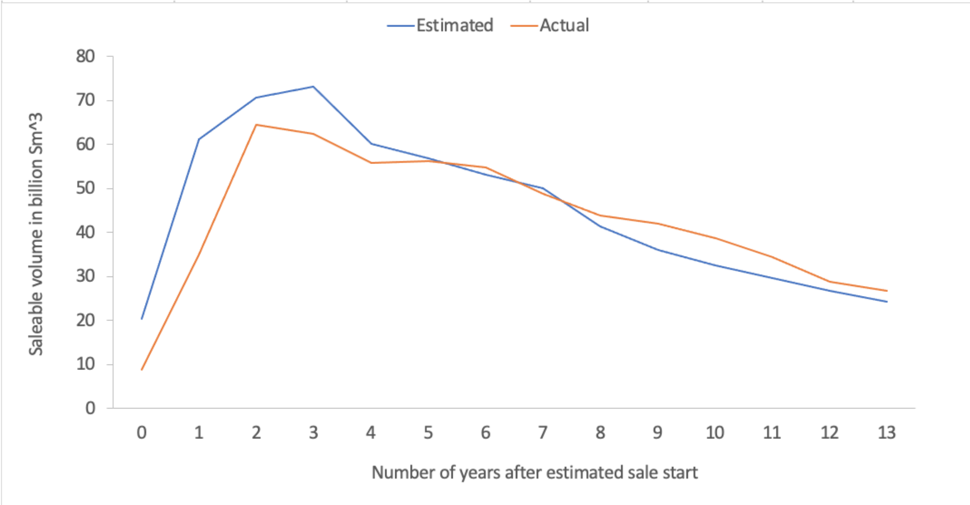

Fig. 1.1.: Annual mean estimate compared to actual

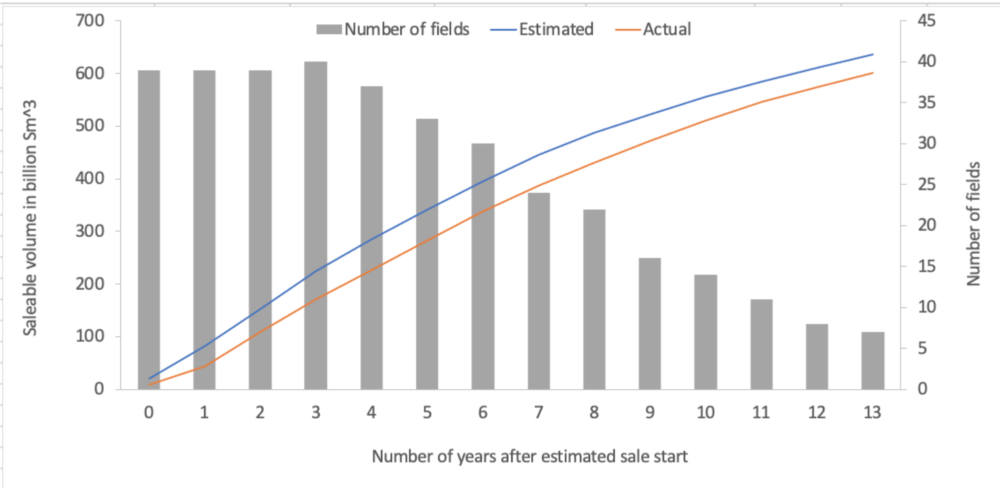

Fig. 1.2.: Accumulated

Fig. 1.1 shows the estimated mean for saleable gas and actual saleable gas after estimated sale start from F0Y to F13Y. We can see that the estimated mean exceeds the actual saleable gas for the F3Y after estimated sale start. From F4Y to F7Y after estimated sale start, we can see both lines are more or less the same, before the actual saleable gas exceeds the estimated saleable gas from F8Y to F13Y. In terms of an economic point of view, we now that NPV have more significance for initial years than later. This is where TVM plays an important role. The concept states the importance of receiving money today than later, because of its potential to expand in value over a specific period of time (Fernando, 2021). Making bad decisions could lead to severe economic loss, and thus, making them correct for the initial years after estimated sale start, could potentially affect the future outcome. Fig. 1.2 presents the accumulated mean estimate for saleable gas and actual saleable gas for 40 fields from Fig. 1.1 we see that the number of fields are decreasing as we go further to the right on the X-axis.

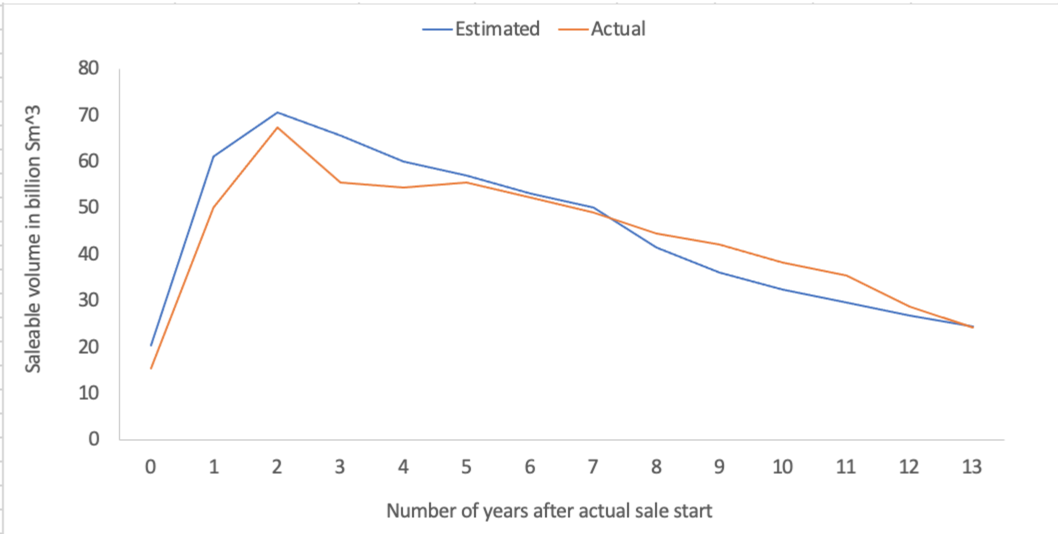

Fig. 1.3.: Annual mean estimate compared to actual

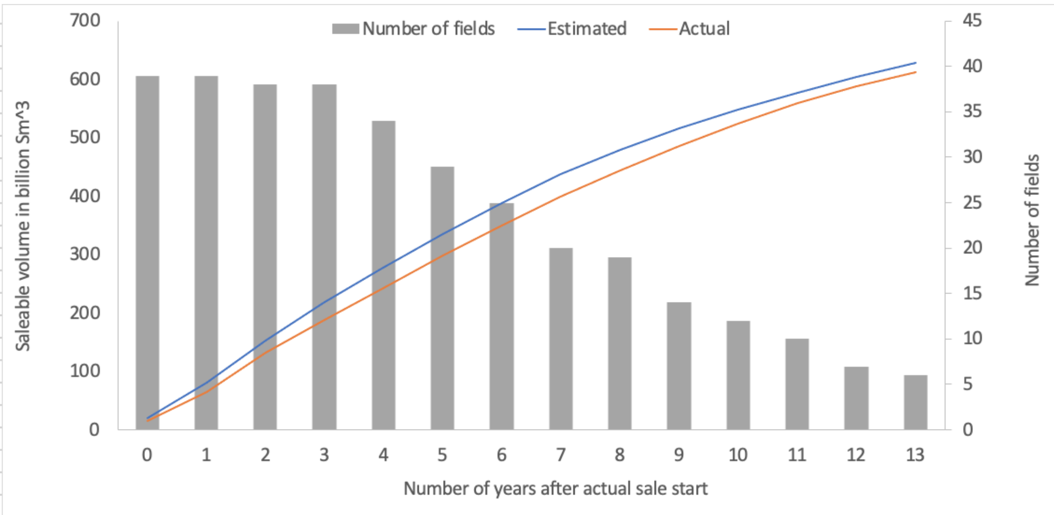

Fig. 1.4.: Accumulated

Fig. 1.3 presents the estimated mean for saleable gas and the actual saleable gas after actual sale start. We see that the estimated mean exceeds the actual up to F4Y after actual sale start. From F5Y to F8Y after actual sale start, we can see that saleable gas estimates and actual saleable gas are more or less the same, before the latter exceeds the first. Finally, for F13Y after actual sale start, we see that both are the same. Ideally, the wish is to achieve this for the entire period, and not occasionally as it is in Fig. 1.3. As mentioned in the previous section, the same economic concept, TVM, can be applied here as well. The intention is to make correct decisions in the beginning, so the economic outcome does not change drastically due to other circumstances. Fig. 1.4 illustrates the accumulated mean estimate for saleable gas and the actual saleable gas for 40 fields. As it was with Fig. 1.2, we see here that the number of fields are decreasing as we move further to right on the X-axis.

1.1 Structure

This thesis will be divided into seven chapters. The second chapter will mainly focus on gas, but at the same time give us some numerical information about oil for fields on the NCS. Chapter three will elaborate the methods used to forecast, and highlight the major reasons for forecasting errors in the petroleum industry. Chapter four will present the raw, RNB dataset, for fields on the NCS, and describe the filtration process of the raw dataset. This dataset will be compared to another dataset, for actual saleable gas, which is collected from NPD‘s website. Moreover, the chapter will describe the methods used to analyse the estimates. In chapter five we will continue with the work done in chapter four, and portray the data at hand with a metalog distribution. The use of this statistical distribution will provide us with more insight and trust regarding the dataset. The sixth chapter will discuss various factors that have lead to the result. Finally, the sixth chapter will summarize the entire thesis.

Background

2

2.1 Total production and saleable

Tab. 2.1.: Annual production in Norway (Petroleum, 2021c))

Year	Oil	Gas	Total	Unit(10^9)
1971	0,000357118	0,102949	0,103306118	Sm^3
1972	0,00192702	0,52736	0,52928702	Sm^3
1973	0,00186952	0,521093	0,52296252	Sm^3
1974	0,002014168	0,557954	0,559968168	Sm^3
1975	0,010995331	2,978395	2,989390331	Sm^3
1976	0,016226786	4,487759	4,503985786	Sm^3
1977	0,016223985	6,522085194	6,538309179	Sm^3
1978	0,020675394	16,68838485	16,70906024	Sm^3
1979	0,023624889	22,83396072	22,85758561	Sm^3
1980	0,03068836	28,16767362	28,19836198	Sm^3
1981	0,029577985	27,74802632	27,77760431	Sm^3
1982	0,030861645	27,75932308	27,79018472	Sm^3
1983	0,038237491	29,95207787	29,99031536	Sm^3
1984	0,04370886	32,4767166	32,52042546	Sm^3
1985	0,047339143	34,19493486	34,242274	Sm^3
1986	0,050579351	34,03355167	34,08413102	Sm^3
1987	0,058538428	34,61873486	34,67727329	Sm^3
1988	0,066881609	36,42326237	36,49014398	Sm^3
1989	0,088266436	39,44663695	39,53490339	Sm^3
1990	0,096843819	37,18897869	37,28582251	Sm^3
1991	0,110513039	39,80626104	39,91677408	Sm^3
1992	0,125936236	42,46462826	42,59056449	Sm^3
1993	0,133770419	41,5955653	41,72933572	Sm^3
1994	0,147673758	45,40345273	45,55112649	Sm^3
1995	0,157926268	47,19046907	47,34839534	Sm^3
1996	0,177361406	59,45754004	59,63490145	Sm^3
1997	0,178388158	70,36492659	70,54331475	Sm^3
1998	0,170038687	72,6097401	72,77977878	Sm^3
1999	0,17069291	80,25499495	80,42568786	Sm^3
2000	0,182125845	90,38480899	90,56693484	Sm^3
2001	0,182070749	95,04142895	95,22349969	Sm^3
2002	0,17339511	107,5209198	107,694315	Sm^3
2003	0,164300546	118,2653753	118,4296758	Sm^3
2004	0,161063213	127,7560881	127,9171513	Sm^3
2005	0,144776181	130,8071173	130,9518935	Sm^3
2006	0,131394	129,852608	129,984002	Sm^3
2007	0,119547941	136,5670921	136,6866401	Sm^3
2008	0,113269684	141,3618123	141,4750819	Sm^3
2009	0,105774732	144,5869873	144,6927621	Sm^3
2010	0,096041739	144,9989119	145,0949537	Sm^3
2011	0,089666887	139,0185258	139,1081927	Sm^3
2012	0,081890627	152,7686886	152,8505793	Sm^3
2013	0,079942432	149,1382628	149,2182052	Sm^3
2014	0,081996501	154,5678167	154,6498132	Sm^3
2015	0,085732212	163,5355354	163,6212677	Sm^3
2016	0,08929808	163,2324254	163,3217235	Sm^3
2017	0,088367782	166,5007489	166,5891167	Sm^3
2018	0,082575421	161,1653946	161,24797	Sm^3
2019	0,078792874	152,9691086	153,0479015	Sm^3
2020	0,09579667	147,7849847	147,8807813	Sm^3

Tab. 2.1 presents the total production of both oil and gas for each year, from the beginning of 1971 to 2020. Essentially, Oil, gas, condensate and NGL, make up for the total production of everything that is produced on NCS. These are excluded from Tab. 2.1, since they do not affect the total production massively. Having said that, we can see that the oil production is much lower than gas. This table summarizes the total production of 117 fields on the NCS. Among these only 28 of them are pure gas fields, while the rest are producing both oil and gas.

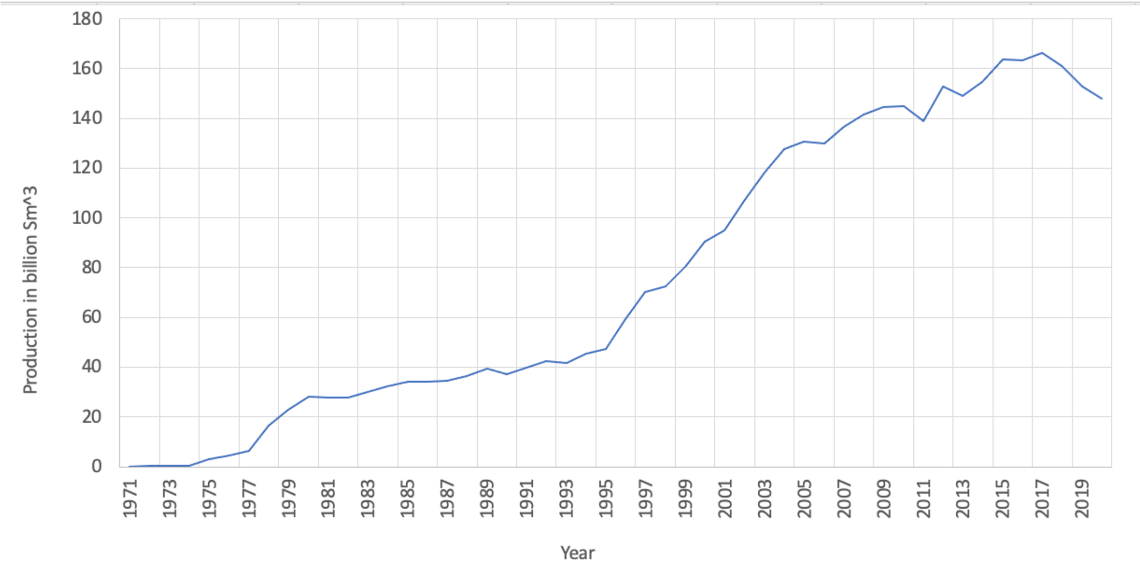

Fig. 2.1.: Total gas production for all the fields from its actual production start

Fig. 2.1 shows a graph for gas production since 1971 to 2020, which is extracted the from Tab. 2.1. The oil production is ignored in this graph, since the numbers are very small compared to gas. We clearly see the increase in gas production from early 1970's till today, which is a consequence of drilling new fields by utilising new technology, and experiences from the past. Different type of gases exist in the petroleum industry. Raw natural gas is combined with different gases. After being separated from oil where applicable, raw natural gas is treated in a processing plant where it is again separated into dry gas components and wet gas components. Dry gas is often described as natural gas, and consists mainly of methane, but also a bit of ethane. Wet gas, or more familiar as, NGL(Natural Gas Liquids), contains of more heavy gases, such as ethane, propane, butane and naphtha. Additionally, we have Condensate, which is another form of gas. (Petroleum, 2021b). In this thesis we are going to work with dry gas because the raw, RNB dataset, contains forecasts for P10, mean, and P90

The total gas production for all fields from its actual production year is shown in 2.2. Placing the gas production for all fields at its actual production start year, is called as year 0(F0Y, and shows that 117 fields(red line) were producing a bit less than 40 billion Sm^3. Additionally, placing the gas production for all fields 1 year(F1Y after production start, shows that 112 fields were producing approximately 130 billion Sm^3. A similar approach does also apply for the remaining years after actual production start as we move to right along the X-axis. The graph reflects the total gas production, which has an increasing trend up to F9Y after production start, before it gradually decreases. The plateau-phase and production shut down for fields are the main reasons for the drop in total gas production some years after production start. In the start-up phase, the fields usually produce more gas as the wells are drilled. After that, the fields go into a plateau-phase, where the production stagnates for some years. For bigger fields the plateau-phase could even last for more years. Thus, the gas production will not exceed the levels as for the previous years. As more years pass after production start, the production of gas falls at a rate of 1% - 10% a year Energies (2015). For instance, fields such as Glitne and Huldra produce for less than 15 years after their first production start. The decrease in number of fields as we move further to right can also be explained as a consequence of plateau-phase and production shut down.

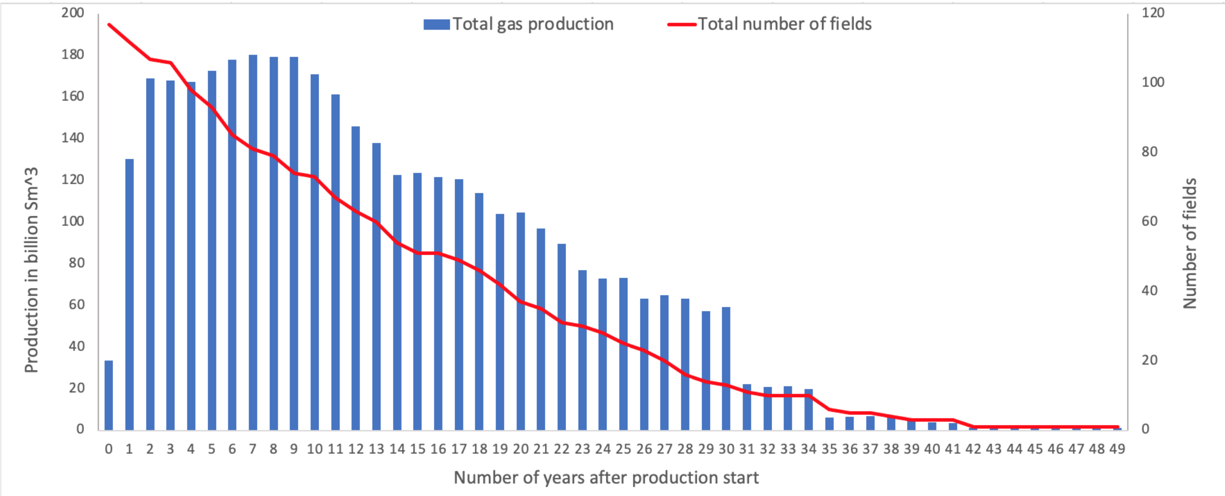

Fig. 2.2.: Overview of total gas production from production start

There are some other fields, which have longer life cycle, and last for many decades after its actual production start. These are considered as large fields, because they produce significantly more gas for a longer period of time compared to other fields. For example, Valhall, Tor, and Ekofisk are large fields that produce for more than 40 years after production start.

Tab. 2.2.: Saleable gas and oil (Petroleum, 2021c).

Year	Oil	Gas	Total	Unit(10^9)
1971	0,000357118	0	0,000357118	Sm^3
1972	0,00192702	0	0,00192702	Sm^3
1973	0,00186952	0	0,00186952	Sm^3
1974	0,002014168	0	0,002014168	Sm^3
1975	0,010995331	0	0,010995331	Sm^3
1976	0,016226786	0	0,016226786	Sm^3
1977	0,016642542	2,65490004	2,671542582	Sm^3
1978	0,020644427	14,20074539	14,22138982	Sm^3
1979	0,022477875	20,6697273	20,69220517	Sm^3
1980	0,02822123	25,08831739	25,11653862	Sm^3
1981	0,027484518	24,95112376	24,97860827	Sm^3
1982	0,028528304	23,96003672	23,98856503	Sm^3
1983	0,035645488	23,61257259	23,64821808	Sm^3
1984	0,041093054	25,96259385	26,0036869	Sm^3
1985	0,044757873	26,18565453	26,2304124	Sm^3
1986	0,048771114	26,08970194	26,13847306	Sm^3
1987	0,05695912	28,1508869	28,20784602	Sm^3
1988	0,064723015	28,32957278	28,39429579	Sm^3
1989	0,085983235	28,73773181	28,82371504	Sm^3
1990	0,094542214	25,47945013	25,57399234	Sm^3
1991	0,108509919	25,02701149	25,13552141	Sm^3
1992	0,123999035	25,83366081	25,95765985	Sm^3
1993	0,131843463	24,80384705	24,93569051	Sm^3
1994	0,14628226	26,84160907	26,98789133	Sm^3
1995	0,156775902	27,81360101	27,97037691	Sm^3
1996	0,175501338	37,39794219	37,57344353	Sm^3
1997	0,175913798	42,94472164	43,12063544	Sm^3
1998	0,168743744	44,19456419	44,36330793	Sm^3
1999	0,168689715	48,47079094	48,63948066	Sm^3
2000	0,181180569	49,79595055	49,97713112	Sm^3
2001	0,180884453	54,03648705	54,21737151	Sm^3
2002	0,173649116	65,59389542	65,76754453	Sm^3
2003	0,165475165	72,95993445	73,12540961	Sm^3
2004	0,162777562	79,31076327	79,47354083	Sm^3
2005	0,148136741	85,84259622	85,99073296	Sm^3
2006	0,136577453	88,66828738	88,80486483	Sm^3
2007	0,128281687	90,30972881	90,4380105	Sm^3
2008	0,122638443	100,079407	100,2020454	Sm^3
2009	0,114969262	104,2460685	104,3610378	Sm^3
2010	0,104415394	106,9978573	107,1022726	Sm^3
2011	0,097460095	101,2663833	101,3638434	Sm^3
2012	0,089200397	114,722961	114,8121614	Sm^3
2013	0,084931506	108,7459985	108,83093	Sm^3
2014	0,087749391	108,3034077	108,3911571	Sm^3
2015	0,090853316	117,0084413	117,0992946	Sm^3
2016	0,093933005	116,7666828	116,8606158	Sm^3
2017	0,092278261	124,6642073	124,7564856	Sm^3
2018	0,086268868	122,203389	122,2896578	Sm^3
2019	0,081756209	115,1232454	115,2050016	Sm^3
2020	0,098414495	112,3023548	112,4007693	Sm^3

Tab. 2.2 presents the saleable oil and saleable gas from 1971 and 1977, to 2020, respectively. By comparing this table with Tab. 2.1, we clearly see that the first sale of gas happened six years after the actual gas production, which was in 1971. By looking at some of the values for saleable oil and saleable gas for different years compared to Tab. 2.1, we can recognize that most of oil and gas that are produced on the NCS, are being sold. This is because Norway is seen as an important supplier of oil and gas. Norway´s production of gas contains up to 3% of world´s demand. Despite the fact that it produces a small percentage, it plays a significant role as an exporting country. Norway is actually the third biggest gas exporter, just behind countries such as Russia and Qatar. Gas is an important energy source in Europe when it comes to heating of homes and cooking. It is utilized as heat and input factor in industry, and additionally, it is used in gas power plants to make electricity. 20% - 25% of the total gas usage in countries that are a part of EU, are delivered by Norway. Almost all gas that is produced in Norway is exported, and the export value accounts for nearly half of total Norwegian export of goods. Norwegian gas deliveries contribute to Europe having a stable and reliable gas supply (Petroleum, 2021a). As mentioned earlier, not all gas is being sold. Gas is also used for other purposes. Among other things, gas is used to generate power in order to drive the fields. For some fields, the gas is also re-injected into the reservoir. The reinforcement is often used in production of oil to maintain reservoir pressure and displace oil. This provides efficient oil recovery, at the same time as the gas is stored for possible recovery later (Petroleum, 2021a).

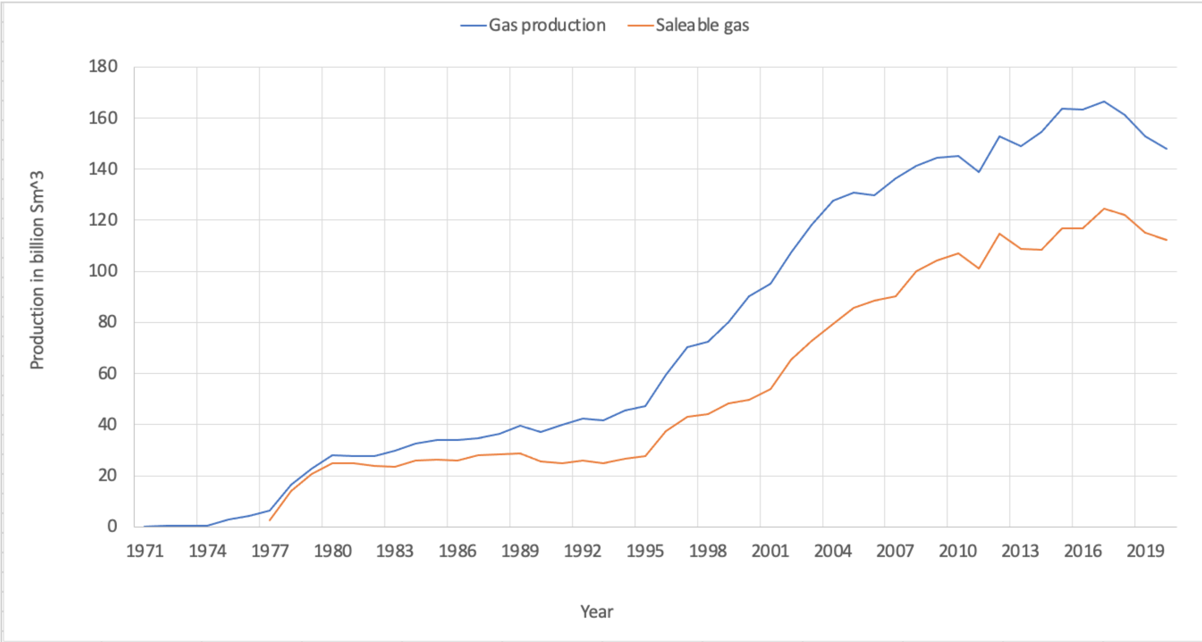

Fig. 2.3.: Comparison of actual gas production and saleable gas over the years

Fig. 2.3 presents the total gas production and saleable gas since early 1970's. In this figure we can see when the actual sale of gas happened, compared to actual production of gas. As it can be seen, the first sale of gas was in year 1977, which was six years after actual gas production. By looking at the graph, we can also see that most of the gas that is produced on the NCS is being sold.

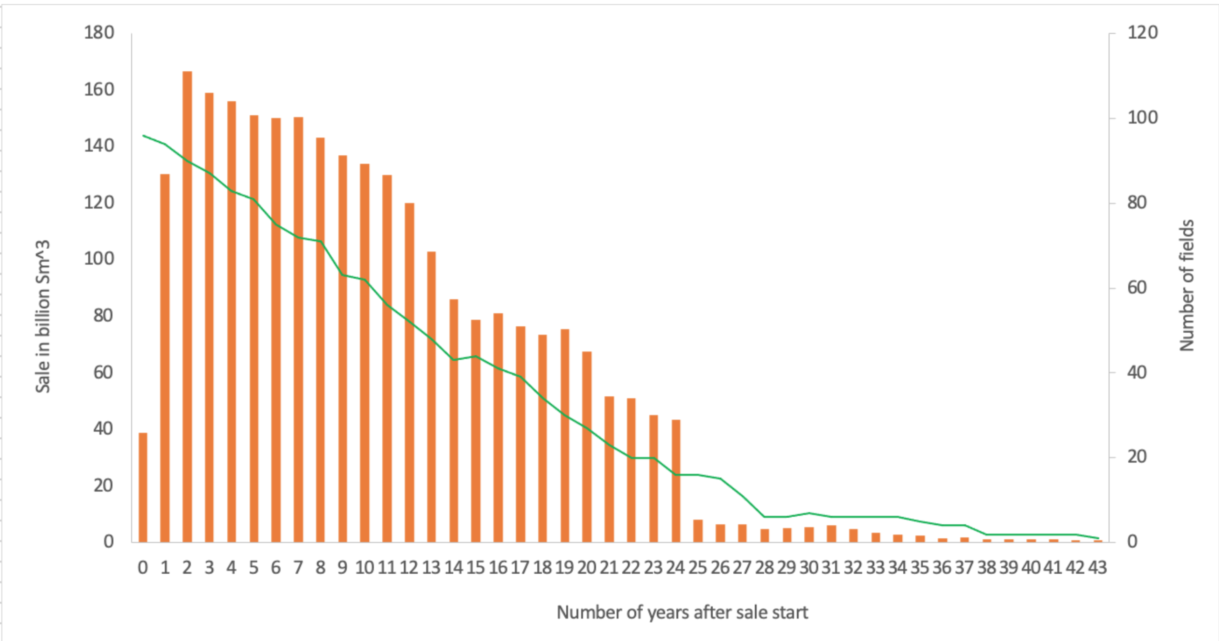

Fig. 2.4.: Overview of saleable from its first sale start

Fig. 2.4 presents the saleable gas for all fields from its actual sale start(F0Y) and further(up to F43Y). The same logic as with total gas production, which was mentioned earlier can be applied here as well. In year 0, we see that operators are selling the gas produced from 96 fields are less than 40 billion Sm^3. As we go further to right on the X-axis, we can see the sale of gas has an increasing trend, and reaches the maximum F2Y after sale start, before it decreases slowly. Additionally, the number of fields are also decreasing as we go further to right on the X-axis. Compared to Fig. 2.2, it should be noted that the operators are selling gas from 96 out of 117 produced fields.

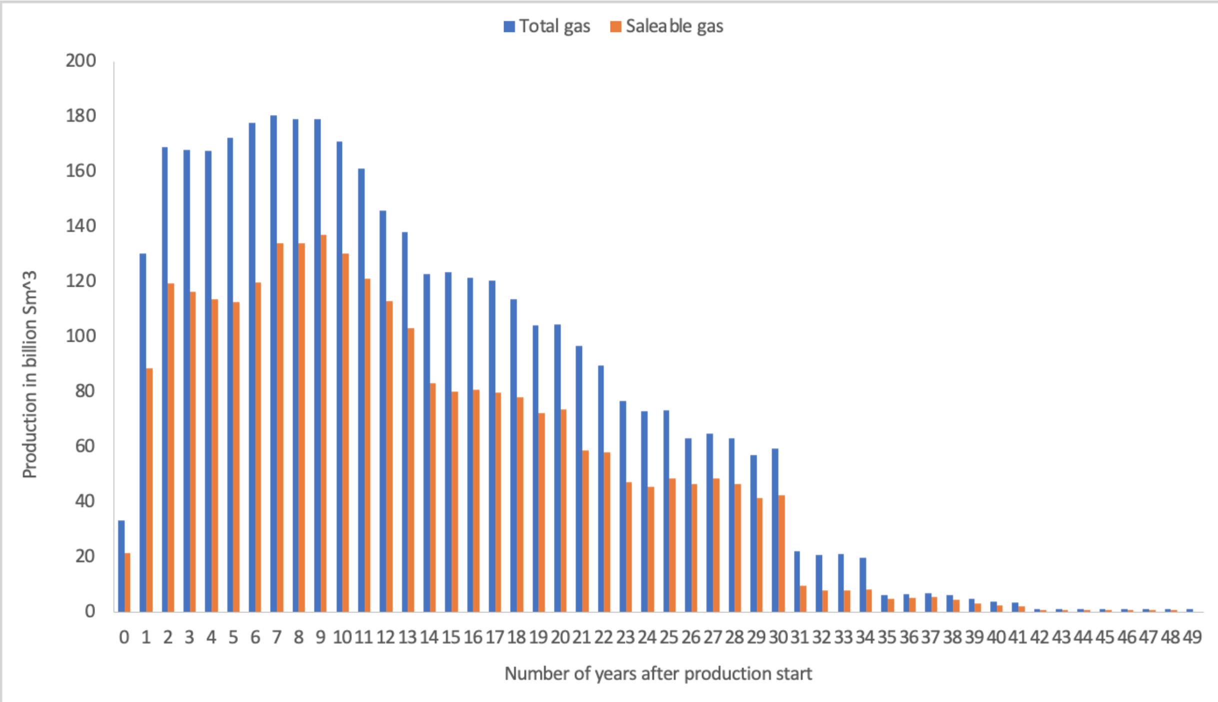

Fig. 2.5.: Total gas production compared to saleable gas from its actual production start

By combining Fig. 2.2 and Fig. 2.4, we get the following graph in Fig. 2.5. The figure shows the total gas production for all fields from F0Y to F49Y after production start(blue bar). The saleable gas(orange bar) is compared to actual production start of gas, i.e. by placing the saleable gas in relation to actual production start of gas. Two two scenarios will be given to illustrate this. For instance, if two fields, X and Y, started its actual production og gas in year 1970 and 1980, and produced 18 billion Sm^3 each, respectively, the sum will be represented as blue bar in year 0. With the first scenario, if field X started its actual sale in 1970, with 14 billion Sm^3, and Y started its actual sale in 1980 with 10 billion Sm^3, the sum is shown as the orange bar in year 0. With the second scenario, if field X started its actual sale in 1971, with 12 billion Sm^3, and Y started its actual sale in 1981 with 9 billion Sm^3, the sum is shown as the orange bar in year 1.

3 Production forecasts in the gas industry

In Norway a Plan for PDO requires probabilistic production forecasts. These can be used a basis for making cash flow predictions, and also as metrics for value-and-decision for NPV and Internal rate of return (IRR). Additionally, the pros and cons of approving a field will be weighed up in terms of uncertainty and economical point of view. The work in this thesis, uses the accumulated probabilistic forecasts for saleable gas made at the time of final investment decision (FID). These will be compared to actual accumulated saleable gas, to investigate whether the forecasts are optimistic, overconfident, both, or neither. According to the guidelines of NPD at the time of FID, the operators should deliver forecasts, such as annual mean, and P10/P90 percentiles for all fields on NCS that are developed (Bratvold et al., 2020). To avoid disasters such as, too much costs compared to revenues, excessive time usage, and delays, perfectly calibrated unbiased forecasts have to be made. In the paper of Bratvold et al., Nandurdikar and Wallace explained that production shortfalls are common, rather than exception.

Next sections will present more insights about the forecasts delivered by the operators. The tools used in the process of generating these percentiles will be explained. Several psychological factors play a huge role when taking decisive investment decision. The common physiological assessment errors regarding forecasts will also be presented since these are very common in the petroleum industry. Finally, the forecasts will be examined in relation to NPD‘s guideline will be explained. The comparison of probabilistic forecasts from the raw, RNB dataset, with the actual saleable gas will tell us whether the operators forecasts meet the NPD‘s guidelines.

3.1 Estimating future gas production

In a perfect world, the actual production should match the forecasted production. However, this is not the case in the petroleum industry. According to Nandurdikar et al., their analysis shows that the production performance has not improved drastically over the years, despite the improvement of technology, and experiences in the past. This negative trend is often referred to optimistic subsurface assumptions, deficiency in processes, and lack of responsibility when it comes to actual production volumes. Having said that, different approaches with advanced computer models are applied to forecast. Having an understanding and information about geological and physical properties of a gas field, will aid the technology through quantitative ideas to develop a field. For the development of a gas field, a reservoir model and a model of a field development process are used as quantitative ideas. Complex mathematical expressions and relationships are used for models and processes when extracting gas from a certain field. The calculations are done through modern computer and computational attainment, which make it possible to illustrate different properties and layers. When utilising modern computer, the expansion of geological, geophysical and hydrodynamic possibilities will be examined. Thus, it will be necessary to build a field development model, based on high level of knowledge about the phenomena dealing with and the requirements that are acceptable (GasWiki, 2021).

Highly developed simulators are utilised in the reservoirs. The common FD simulation is dependent of three physical theories about: conservation of mass, isothermal fluid phase behavior, and the Darcy approximation of fluid flow through porous media. Various techniques are often utilised in modern simulators. FD simulation provides 3D representations in either full-field or single-well models. Natural fracture simulation is another technique, which has an exceptional feature, and models hydrocarbons in compact matrix blocks. The flow comes from compact matrix blocks to a higher permeable fracture network that binds the blocks and the wells. A compositional reservoir simulator measures the PVT properties of gas and oil phases. The aim is to dynamically record the movement of both phases and components in fields. This is done at the expense of expanded cost in terms of setup time, compute time, and computer memory (GasWiki, 2021).

3.1.1 PDO

PDO is a document delivered by the operators before a field is approved for production. This document must fulfil some specific guidelines, which address points that must be included in the assessment. In drilling and well activity, the points below should be included in the document (of Petroleum & Energy, 2018):

- Purpose and schedule for the planned drilling and well activities
- References to relevant governing documentation for the respective activities
- Overview of deviation in relation to regulatory requirements and internal procedures/requirements
- Description of the planned drilling and well activities, with associated use of downhole equipment, surface equipment and safety valves
- Well sketch with clear indication of barriers in connection with drilling and well activities and technical solutions for completion and permanent plugback of the well
- Summary of potential technical and operational problems that can occur during the activities, identified risk, as well as precautions planned in this connection
- Geological forecasts and information of significance for the activities
- Account of any planned use of oil-based drilling fluid
- Plan for disposal of drilling cuttings

The PDO takes into account the development of a petroleum occurrences, and the importance of the planned development measures. This must again be approved by the Ministry of Petroleum and Energy (MPE). The decisions are based on quantitative- and qualitative assessments (of Petroleum & Energy, 2018).

3.1.2 Uncertainty

Predicting numerical values of an event in the future could be a hard task, since it is connected to uncertainty. This is also the case in the petroleum industry, where several known factors, and sometimes, even unknown factors are involved. Forecasts for gas in the petroleum industry are generated with different degree of uncertainty. Below, a general structure for different phases of forecasting in the petroleum industry is illustrated:

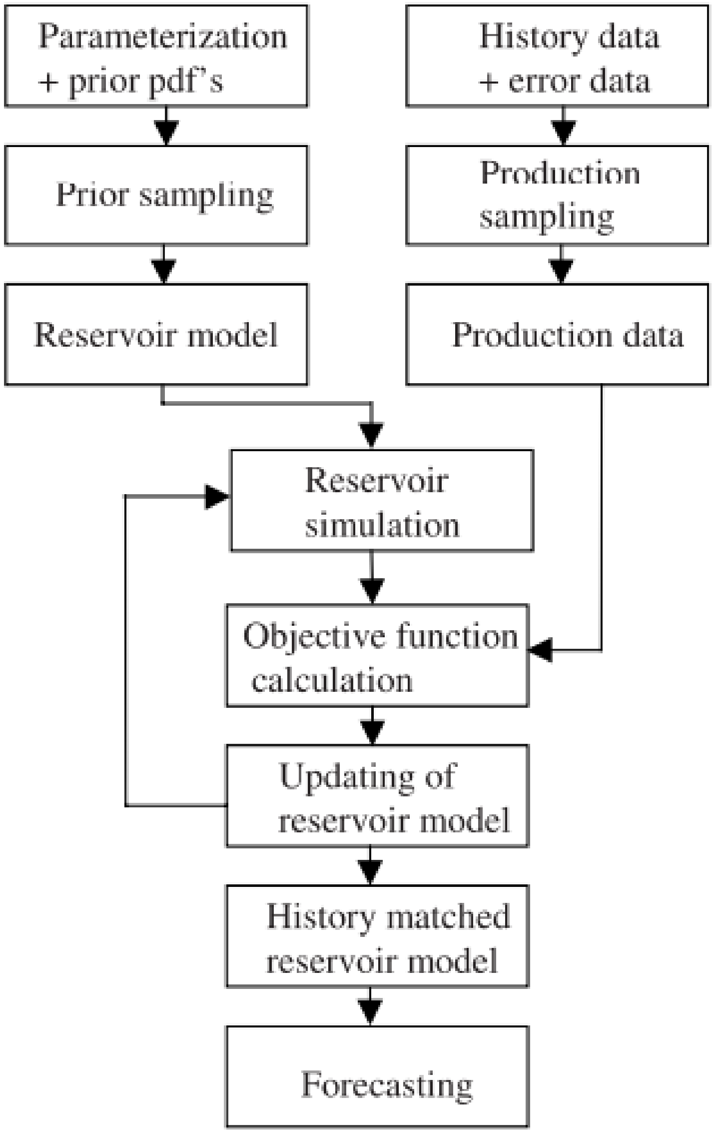

Fig. 3.1.: A flow chart diagram used for quantification of forecasting uncertainty (Floris et al., 2001)

The development of reservoirs is dependent of production forecasts from the historical values of an identical reservoir model (Floris et al., 2001). In uncertainty analysis within production forecasting, finding low-, best- and high productions forecasts are common. These forecasts can be generated with either probabilistic and deterministic methods (PetroWiki, 2021). These methods differ from each other in the way they deal with uncertainty as input parameters when constructing a model. A deterministic approach ignores fluctuation in the input parameters with time, and rather concentrates on estimating probabilities of different outcomes if possible. A decision tree is used for forecasts in a deterministic model. On the other hand, a probabilistic method accepts that a estimate can't be 100% precise, and illustrates possible values as a function of statistical distributions. Monte Carlo simulation is a familiar tool that is used for probabilistic models (Siddiqui et al., 2007).

When analysing uncertainties, establishing a way to distinguish complex forecasts into static or dynamic components can be helpful when calibrating them individually. However, controllable, and operational uncertainties could be important in the later stages, and thus, these must be available for further uncertainty analysis or decision analysis. Having said so, the procedure to quantify each uncertainty is not always so simple. Categorizing each individual uncertainties into components, e.g. measurement or model, and looking into portfolio and sample-bias can be supportive when constructing a range of values for each uncertainty. However, uncertainties related to geological aspect could be problematic to work with as continuous variables. Therefore, discrete models for geological aspect have to be established to present the range of possibilities. Likelihoods have to be assigned to each model when integrating continuous parameters and generating outcome distributions. An advantage with a discrete model is that values are based on a scenario which are consistent and reliable, rather than working with independent geological-parameter values that are meaningless. Having said that, frequent verification of the available data set is important. This is because many studies indicate that people often anchor on their gut-feeling, and therefore miscalculate uncertainties due to lack of frequent verification of the available data set. Thus, having any quantitative data is key when establishing and validating uncertainty interval (PetroWiki, 2021).

It is important to establish distributions for each uncertainty as well. Adapted probability distributions are well-behaved and easier to establish. By well-behaved, we mean that the distributions are bounded, and easier to establish, where the distributions are either uniform or triangular. Generally, establishing range of values has more impact on forecasts than the specific distribution shape. Thus, the correlation among uncertainties should be examined (PetroWiki, 2021). As mentioned in the previous section, Monte Carlo Simulation is a useful tool when generating production forecasts. The tool helps to generate output percentiles, such as P10, P50 and P90, which we will look at soon.

Lot of researches and experiments have been done regard to uncertainty reduction over the past decades. Despite that, the are concerns regarding the production forecasts today. The word *uncertainty* was unheard of at around mid-1980's, when one of the authors worked on production forecasts on the NCS (Bratvold et al., 2020). Fig. 3.2 shows statistics of papers published in relation to probabilistic production forecasts.

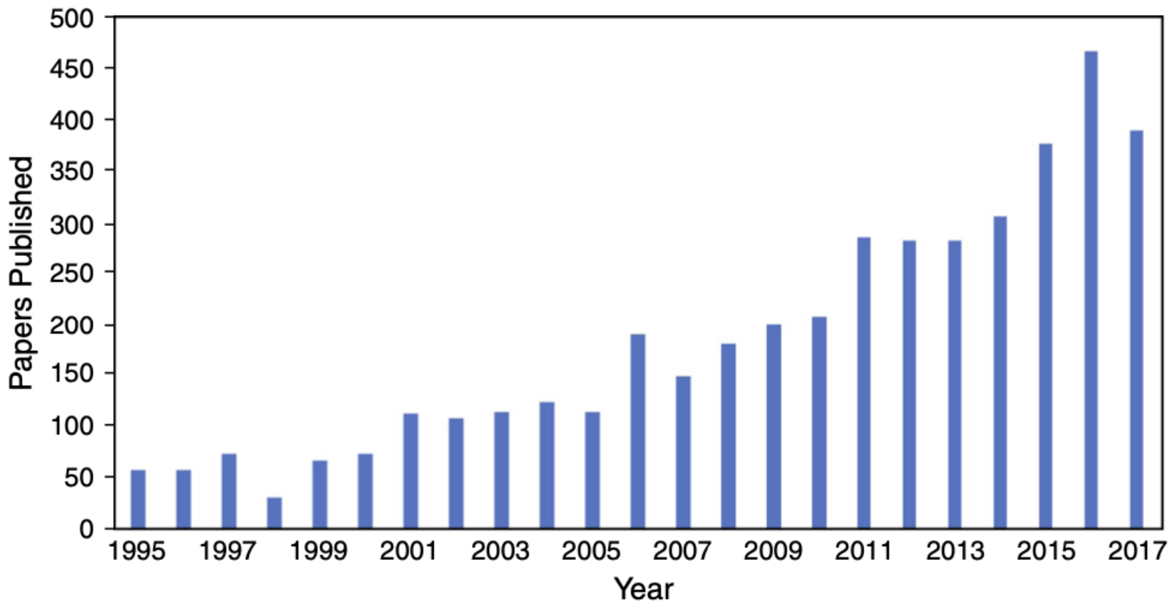

Fig. 3.2.: Increase in number of papers regarding probabilistic production forecasting from 1995-2017 (Bratvold et al., 2020)

The question to be asked is, whether the operators learn from their flaws in the past. Despite the increase of number of paper published in relation to production forecasts, over a time span of 22 years, from 1995-2017, the petroleum industry is still struggling with the deviation between the forecasted production values and the actual production values. In fact, from the researches of Bratvold et al., the number of papers in relation to probabilistic production forecasting has increased by more than 600% in that period.

3.1.3 P10, P50 and P90

There are clear guidelines from NPD on how to interpret percentiles such as P10, P50, and P90. Below, the guidelines on how to interpret probabilistic forecasts are given:

Uncertainty category	Definition	Explanation
Low estimate (L)	Low estimate of petroleum volumes that are expected to be recovered from a project.	The low estimate must be lower than the base estimate. The probability of being able to recover the indicated estimate or more must be shown (e.g. P90). Compared with the base estimate, the low estimate should express potential negative changes with regards to mapping of the reservoir, reservoir/fluid parameters and/or recovery rate.
Base estimate (B)	Best estimate of petroleum volumes that are expected to be recovered from a project.	The base estimate must reflect the current understanding of the scope, properties and recovery rate of the reservoir. The base estimate will be calculated using a deterministic or stochastic method. If the base estimate was calculated using a stochastic method, the base estimate shall be stated as the expected value.
High estimate (H)	High estimate of petroleum volumes that are expected to be recovered from a project.	The high estimate must be higher than the base estimate. The probability of being able to recover the indicated estimate or more must be shown (e.g. P10). Compared with the base estimate, the high estimate should express potential positive changes with regards to mapping of the reservoir, reservoir/fluid parameters and/or recovery rate

Tab. 3.1.: Definitions for the estimates according to NPD´s guidelines Petroleum (2020)

Tab. 3.1 presents the explanations regarding uncertainty from NPD. It should be noted that, in this thesis the low estimate is referred to P10, and the high estimate is referred to P90. The points mentioned below tell how the percentiles are interpreted in this thesis:

- P10: There is at least 10% probability that the actual value is less or equal to the low estimate
- P90: There is at least 90% probability that the actual value is less or equal to the high estimate
- P50: There is at least 50% probability that the actual value is less or equal to the best estimate

3.2 Reasons for forecast errors

This section will address the common psychological factors involved in decision-making. Ideally, the forecasts have to be *unbiased*. This is not the case in the petroleum industry in Norway which is heavily influenced by *biased* decisions. Nandurdikar and Wallace explain that production shortfalls are a habit rather than exceptions based on historical experiences (Bratvold et al., 2020). According to Flyvbjerg, *bad luck*, *deception* and *delusion* are the main reasons for forecasting errors. This section will elaborate on these three key words.

3.2.1 Bad luck

Bad luck is referred to poor or unexpected results by the management. Although, unexpected events could happen, very often, a poor outcome is a result of several psychological aspects involved. Diversity of scope changes, complexity in reservoirs, accidental geological features can be regarded as bad luck during a project (Flyvbjerg et al., 2009). Black swan is a term related to unforeseen outcome and is connected to bad luck. This concept has got much attention when it comes to risk and safety over the years. According to Aven, black swan is seen as surprisingly extreme event relative to one´s belief/knowledge. According to him, there are mainly three types of black swan events (Aven, 2015):

- Events that were completely unknown to the scientific environment (unknown unknowns)

- Events not on the list of known events from the perspective of those who carried out a risk analysis, but known to others (unknown knowns – unknown events to some, known to others)

- Events on the list of known events in the risk analysis but judged to have negligible probability of occurrence, and thus not believed to occur

In the petroleum industry, if a poor outcome is a consequence of bad weather, this cannot be referred to as bad luck. The management should know better about the weather condition, and find possible solutions to avoid poor outcome. Referring to bad weather is acceptable once. However, if it happens many times, it is because of poor assessment and bad decision-making by the risk analyst.

3.2.2 Deception

Deception is used to explain the flaws behind a decision-making. These flaws are mainly connected to political and agency related decision-makings in megaprojects. Often, these flaws come as a consequence of a strategic misinterpretation and biased decision-making in first place, where a benefit can be gained. This is where the principal-agent problem occurs, where the agents act on their behalf by carrying out tasks. They make sure that their advantages are increased for their projects, and not for their competitors. For instance, projects with huge investments do usually have multiple tiers which are exposed to P-A issues between every two levels of a management (Flyvbjerg et al., 2009).

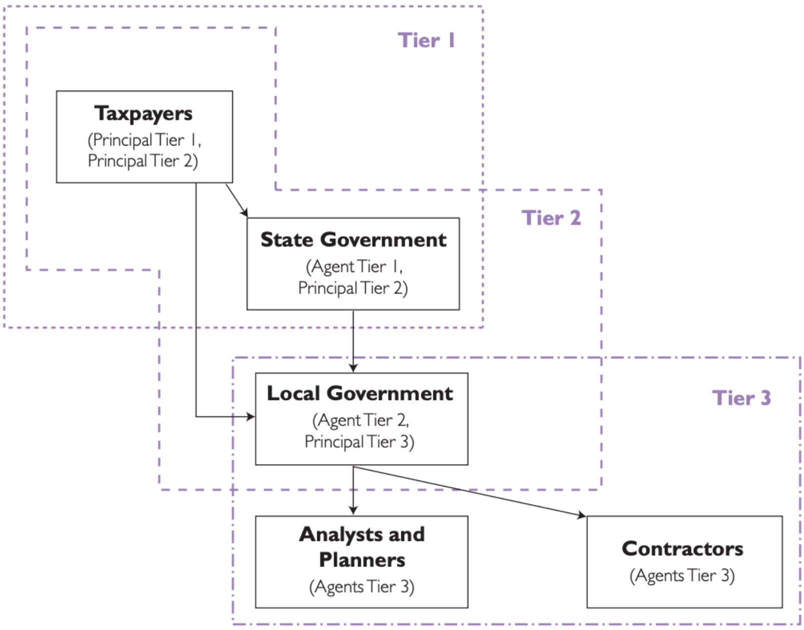

Fig. 3.3.: Overview of three P-A tiers for a megaproject (Flyvbjerg et al., 2009)

Fig. 3.3 shows a typical principal agent system. In the different parts of this P-A system, benefits are achieved through strategic misinterpretation of tempting incentives and other attractive options. The first tier shows the relationship between the taxpayers(principal) and the state government(agent). These two can have different views in relation to their interests. For instance, the government could prefer to act according to their interest, which could possibly be that the projects are developed within the acceptable amount of CO_2 emissions. On the other hand, taxpayers would most likely increase their benefits by lowering the cost and risk, and get it done within their wished timeline (Flyvbjerg et al., 2009).

In the second tier, a disagreement could occur between the operator and the government. As the operators are preparing for the PDO and have the knowledge and insight about a megaproject, they could play with the numbers and other relevant details so that they can gain benefits, and highlight it more, despite the risk and costs associated with that project. On the other hand, this does not necessarily fulfill the criterion from the government´s side. A conflict like this could potentially influence the final results, as these are not resolved at the initial stages. Although, tiers could drastically change from their plan in the beginning, these are still needed for megaprojects in order to complete them properly (Flyvbjerg et al., 2009).

3.2.3 Delusion

Delusion is another forecasting flaw due to psychological dominance in the decision-making. The decision makers are more attracted to the potential of a project in the future, rather than weighing it up against realistic benefits, losses, risk and probability. This is often related to delusional optimism, where they put ideas of future success ahead of realistic hurdles, when it comes to mistakes and miscalculations. By looking back at these errors, one can understand that these biases are a consequence of taking an inside view in forecasting. Instead of assessing the project as a whole, and plan for a long-term, the decision makers have the tendency to overestimate and put their attention on specific issues which they consider as unique to find a solution in the short-term (Flyvbjerg et al., 2009). According to Kahneman and tversky, this what they call the planning fallacy and optimism bias, where the mindset of the decision makers is to underestimate cost overruns, scheduled time, and production compared to their assumptions in the beginning. Overoptimism is related to cognitive bias, and is about the way they interpret information. This can be reduced by consulting other colleagues within the organization to see how many of them are supportive to a decision-making, which at worst could lead to poor investments and waste of time (Flyvbjerg, 2007). Taking a rather an outside view of the potential issues may help to reduce the effects of delusional decision makings (Flyvbjerg et al., 2009). Having said that, delusional bias forecasts can be categorized into four subcategories, which are related to projects within petroleum industry. These are information availability, anchoring, overconfidence, and trust heuristics.

3.2.4 Information availability

As Bratvold et al. have discussed, the issue in relation to decision-making occurs due to lack of ability from human beings to gather and understand new information. Understanding information is an important building block for making decisions, and the availability of information could possibly lead to cognitive bias. Having said that, the quality of information is also an important factor to consider. Very often, personal experiences and insights about uncertainty, and preferences can be a hurdle and deluding. Decision makers tend to use their experiences from different settings and situations, and through the influence of media, in a project which could possibly end up as a disaster. Therefore, having an understanding about their limitations of understanding information is vital. This is important when several variables must be included in the decision-making process, which they forget at the beginning of a project. As Bratvold et al. have discussed, decision makers tend to take the so-called "shortcuts" that give them false expectations and poor intelligence. By nature, they tend to believe in the first available information and accept statistics or paragraphs of text. Good results and experiences from a previous project can overshadow the real circumstances of a new project, and make the decision maker feel confident. The new project may possibly differ from the previous one in terms of foundation, scope and risk.

3.2.5 Anchoring

Anchoring occurs when the decision maker takes an inside view of a project, which leads to optimistic forecasts (Flyvbjerg et al., 2009). This happens when decision maker relies too much on base estimates they have at hand, independent of its importance and the wide range of uncertainty. Although they know that their estimates are too high or too low, they still lack the ability to be closer to the real value. This is a very common tendency among the employees in the oil and gas industry. Experts with high knowledge and expertise are less prone to anchoring than a non-expert in a similar area (Welsh et al., 2005).

3.2.6 Overconfidence

Overconfidence is probably the most familiar cognitive bias among employees in the oil and gas industry (Welsh et al., 2005). Very strangely so, this tendency exists in the nature of human beings, since they prefer to go for favourable choices in relation to their knowledge and intellectual abilities. This tendency makes them overestimate their knowledge and intellectual abilities (Bratvold et al., 2002). The most concerning part, is that people who are respected and appreciated for their knowledge and accurate thinking often fall in the category of being overconfident. In the oil and gas industry a 80% confidence interval is constructed to explain estimates of geological variables in the reservoir. The actual value for the fields should be 80%. However, based on the data for the fields, on average the actual value is less than 50% (Welsh et al., 2007).

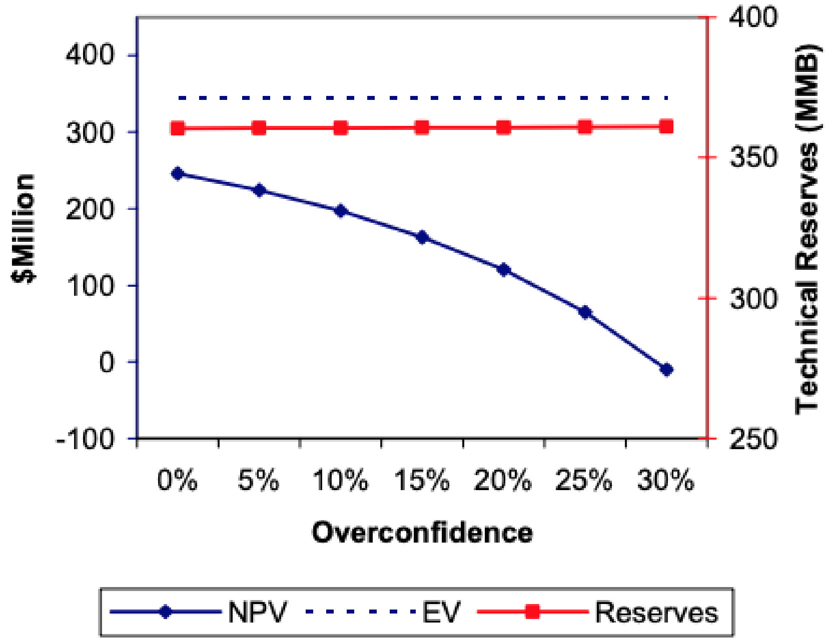

Fig. 3.4.: Overview of the result of overconfidence on NPV in a project (Welsh et al., 2007)

Fig. 3.4 reflects the economic result of being overconfident. The mean NPV for 10 000 iteration from a simulation of a project is shown for different levels of overconfidence. It can be seen that the EV and the reserves for a project remain the same. However, the simulation for NPV does not match the levels of EV as we move further to right on the X-axis. Even at 0% the NPV is only $246 million compared to EV, which is $346 million. This can be explained due to the results arising from the complexity of the model. Moreover, the decline of NPV is very clear as the percentage of overconfidence increases along the X-axis. In fact, at 5% overconfidence the NPV reaches to $224 million. Even Further, at 30% overconfidence the project gets a negative NPV of $-10 million. As a consequence this, the expert who is 30% overconfidence would conclude that the NPV of the project is $246 million, while the actual NPV would reach $-10 (Welsh et al., 2007). In conclusion, the effect of overconfidence could possibly lead to severe economic loss. Thus, it is vital to reduce the degree of overconfidence in relation to one´s knowledge and intellectual ability, by accepting what they know, and strive to understand what they do not know about.

3.2.7 Trust heuristics

Trust heuristics is also a cognitive bias, which is familiar in the oil and gas industry. This works slightly in a different way, since this diminishes the approaches to avoid becoming overconfidence. In the petroleum and gas industry, the trust heuristic can be explained as a trend where the managers rely on the judgements of specific individual(s) without giving a chance, listening or discussing with other colleagues in the same team/group. One can argue that the trust of managers on certain individuals should be based on their exceptional work. Even then, one can argue that listening to multiple ideas and different standpoints can enhance the trust, rather than trusting the work of a certain individual or a group (Welsh et al., 2007).

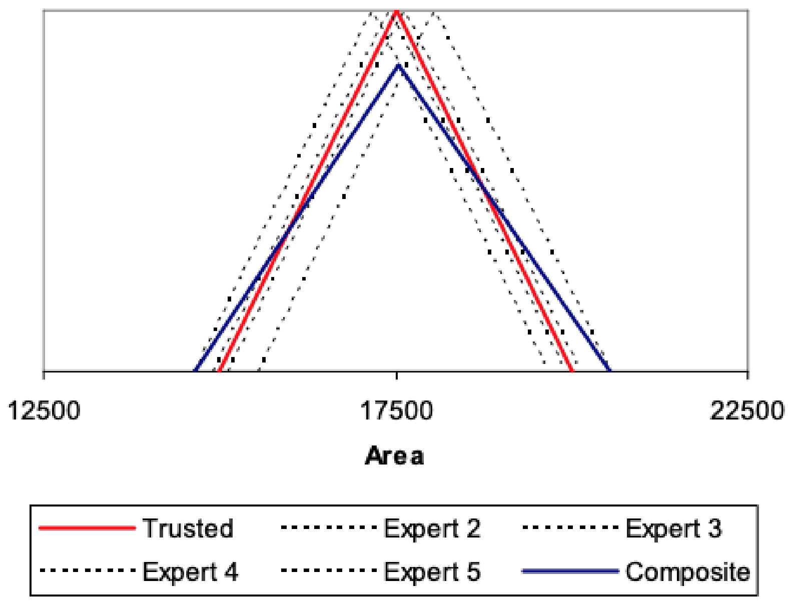

Fig. 3.5.: Opinions from single expert VS multiple experts (Welsh et al., 2007)

Fig. 3.5 presents a scenario, where the information of several experts are compared one trusted expert. The figure shows the opinions of five experts by presenting a triangular probability density functions (PDFs) for an uncertain input parameter value of an area. The lines indicate the experts competence to reflect the differences in accuracy compared to each other. The managers rely on the red line(trusted) in this case. The premise is that the most central of the experts judgements are concrete, and as a consequence of that, the managers are determined to trust them. Comparing the "trusted" distribution to the composite distribution of the five experts, we can see that the "trusted" distribution(red line) is more compressed than the composite distribution(blue line). It tells that the experts are quite careless when estimating the possible range of an uncertain parameter value of an area. On the other hand, if the managers focus on the wider composite distribution(blue line), by putting more trust on to them, they are more credible to present more accurate information (Welsh et al., 2007).

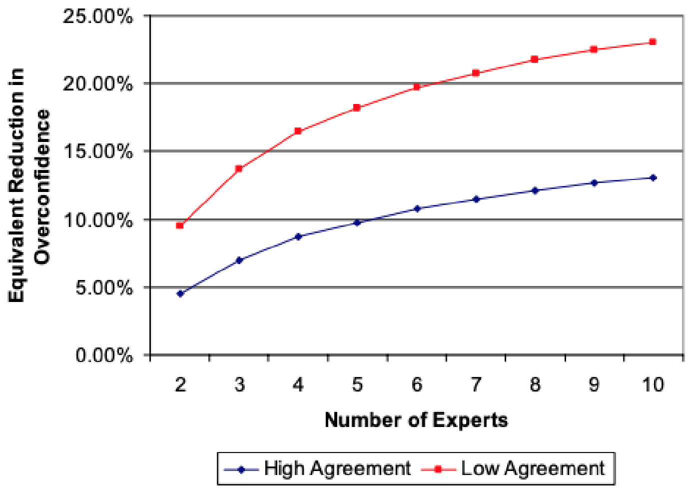

Fig. 3.6.: Graph on the reduction of overconfidence by numbers of experts and level of agreement (Welsh et al., 2007)

Fig. 3.6 presents a model from Welsh et al., which illustrates trust heuristics regarding overconfidence. Their model considers two to ten experts for both high and low degree of agreement, and presents the mean results after doing 10 000 iterations. It can be seen from the model that, addition of a single expert equals of reducing overconfidence up to 5% when the agreement is high and nearly 10% when the agreement is low. Increasing the number of experts to ten diminishes overconfidence in the trusted expert´s distribution to 14% for high agreement and approximately 23% for low agreement (Welsh et al., 2007).

In terms of an economic point of view, one can see the results of trust heuristic by comparing both figures above. Considering the case with overconfidence, from Fig. 3.4, a 5% shift in overconfidence could correspond to huge error in the calculation for the NPV of a project between $22 and $75 million. This depends on the expert´s degree of overconfident to start with. In conclusion, although this sections does not cover the whole story regarding issues in the oil and gas industry, the numbers clearly show that they still have a lot of work to do. They should be much better at utilising their knowledge and consider opinions from different experts within their field of expertise (Welsh et al., 2007).

3.3 Perfectly calibrated forecasts

Historical data for actual outcomes and forecasts are needed to evaluate the performance of the operators ability to deliver unbiased forecasts. These are essential to enhance bad outcomes from the past into positive outcomes in the future. To do so, a statistical distribution can be utilized. The main work in this thesis is to investigate whether the operators provide well-calibrated forecasts for the development of fields on the NCS. To investigate that, the operators production forecasts will be compared to unbiased forecasts. The conditions below have to be fulfilled for the production forecasts delivered by the operators to be classified as well-calibrated forecasts (Bratvold et al., 2020):

1. The range of actual production outcomes falls within the range of predicted production outcomes. However, if too many actual production outcomes fall outside the range of predicted possible outcomes, the forecasters are overconfident. For the production forecasting context evaluated in this paper, approximately 80% of the actual production outcomes should be within the forecasted P10/P90 range.

2. The average of the forecasted production rates should be close to the average of the actual production rates. If this is not the case, the forecaster is either optimistic or pessimistic

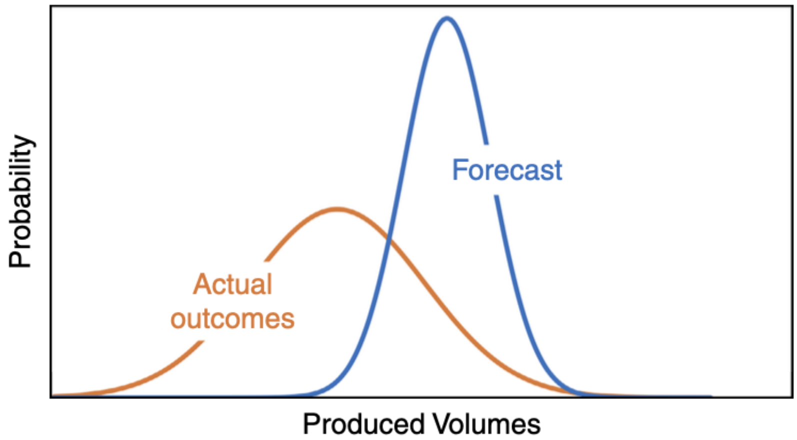

Fig. 3.7.: Forecasted and actual outcome for produced volume (Bratvold et al., 2020)

The production forecasts are heavily influenced by optimism and overconfidence. To illustrate that, Fig. 3.7 shows a case of these biases with random data for produced volume over a certain period of time (Bratvold et al., 2020). The forecaster´s degree of optimism and overconfidence is illustrated by Fig. 3.7, which shows the mean produced volume for a limited amount of fields. The means of both forecasted and actual outcomes are plotted, respectively as blue and orange. We see the forecasted range is smaller compared to the actual outcomes, which deviates from the 1.st criteria for the well-calibrated condition above, and indicates that the forecaster is overconfident. Moreover, the forecasted mean is clearly greater than the mean of actual outcomes, which deviates from the 2.nd criteria for the well-calibrated condition above, and proves that the forecaster is optimistic (Bratvold et al., 2020). A scatterplot can be used to compare the forecasts with the actual outcomes. How well the forecasts are can be assessed by Fig. 3.8 using random data. The figure shows forecasts for P10, P50, and P90. Ideally, the P50(blue dots) forecasts have to lie between the P10:P90(error bars) forecasts for 80% confidence interval. The Y-axis shows the actual results, and the X-axis shows the estimates. To investigate whether the forecasts are unbiased the following conditions below have to be fulfilled (Bratvold et al., 2020):

1. Approximately 50% of the P50-markers are to the left and to the right of the 45-degree line(red line)

2. Approximately 80% of the P10:P90 confidence intervals would contain the associated actual value, i.e. touch the red line. If not the forecaster is either optimistic or pessimistic

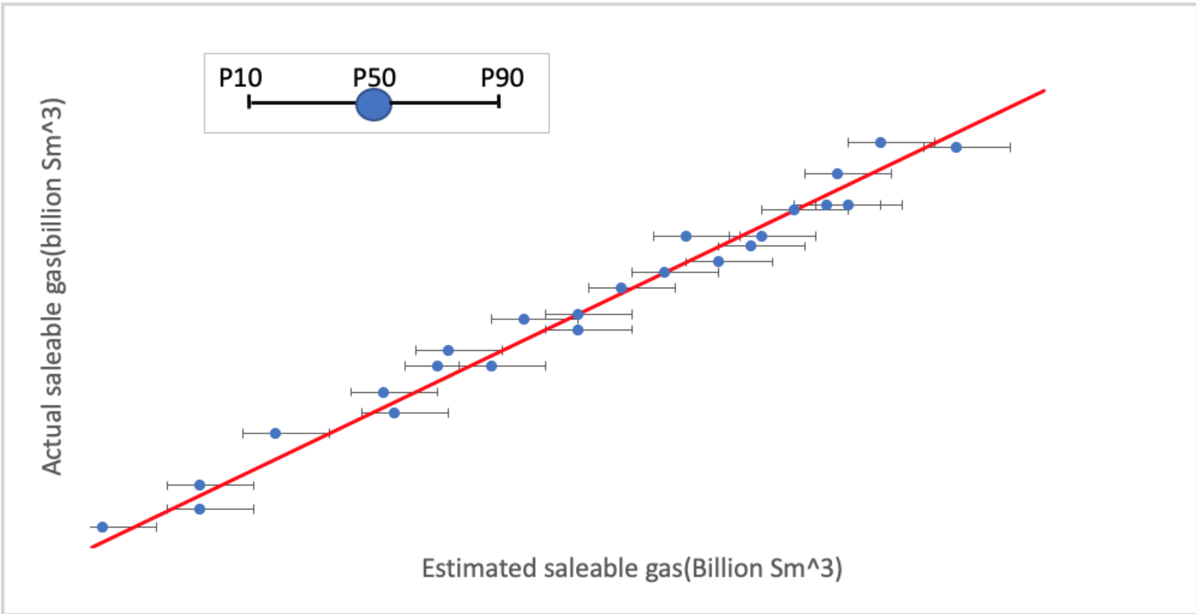

Fig. 3.8.: Ideal scenario

If the percentiles do not touch the 45-degree line at all, it will indicate a high degree of overconfidence by the operators. With synthetic data from Fig. 3.8 we can see that all the percentiles are touching the red line, which is a good sign. If the P50(blue dots) fall below the 45-degree line, this will indicate optimism by the operators. On the other hand, if the P50 fall above the 45-degree line, it will indicate pessimism (Bratvold et al., 2020). Note that the axis titles for Y-axis and X-axis state "Estimated saleable gas" and "Actual saleable gas", respectively. Although we have portrayed the situations for the forecasted and actual outcomes for produced volume, the criteria and the figure also apply for saleable gas.

4 Dataset

This chapter will inspect the data for actual saleable gas, and the raw Revised National Budget (RNB) data for estimated saleable gas that are provided by Norwegian Petroleum Directorate (NPD) for all the fields that have got PDO approval since year 2000. More specifically, the actual accumulated saleable gas will be compared to accumulated forecasts for saleable gas. Two methods are utilised to compared them. With the first approach, the actual data is normalised to estimated data, and delay will not be considered. With the second approach, the estimated data will be time shifted, and compared to actual data, which will consider delay. Data for actual saleable gas can be collected from the NPD's website. On the other hand, the saleable gas estimates provided by the operators at the time of final investment decision (FID) are given through a confidentiality agreement with Norwegian Petroleum Directorate (NPD). Thus, any field name or specific data values due to agreement on confidentiality, will not be mentioned in this thesis. In case a field and its associated information is mentioned, this is due to the public availability. Furthermore, occasionally for some graphs, values on the Y-axis will be hidden in case they are transparent and reveal information about certain field(s). In this thesis, we are going to focus on First zero year (F0Y) to First thirteen years (F13Y) of saleable gas. The coming sections will describe the obtained raw RNB dataset from NPD. This chapter will mainly focus on the process of filtering out the inconsistent estimates, and follow up with the two methods used to analyse these estimates.

4.1 Description of the dataset

As mentioned in the previous paragraph, the dataset contains confidential information at a field level for both saleable dry gas and saleable oil on the NCS provided by Norwegian Petroleum Directorate (NPD). The dataset consists of 292 852 rows with information about oil and dry gas. In the dataset, we can find field names, the different estimates, i.e P10, mean, and P10, forecast start years for fields, updated forecasts, and so on. Additionally, there are in total 113 fields, which contain both annual- and accumulated estimates. The unit for dry gas and oil are in billion and million Sm3, respectively. If we separate them, we can find 109 fields with 192 299 estimates(annual and accumulated) for saleable oil. On the other, there are 105 fields with 100 553 estimates(annual and accumulated) for saleable dry gas.

4.1.1 Filtration process of the dataset

As the main purpose of this thesis is to focus on saleable dry gas, we will from now on exclude everything that has to do with saleable oil, and solely focus on dry gas. Separating the 100 553 estimates(annual and accumulated) leave us with 40 751 annual estimates and 100 fields. We have 59 802 accumulated estimates and 98 fields. Initially, the operators provided reports for both annual- and accumulated estimates. The annual estimates are supposed to describe the yearly uncertainty in geology, while the accumulated estimates are supposed to include uncertainties related to operational issues. However, since 2016 the operators only reported the annual estimates as they recommended these over the accumulated estimates. The main reason for this is because the annual estimates are more representative forecasts by the companies.

In this thesis we are going to work with the accumulated estimates due to a larger portion of data points at hand. These will provide us better interpretation of the results, rather than using the annual estimates. Thus, excluding the annual estimates give us 59 802 accumulated estimates and 98 fields. As mentioned earlier, we are going to work with fields that have got PDO approval since year 2000 and later. The next step is to extract the accumulated estimates for each field from its PDO approval year. Doing so, reduces the dataset significantly to 13 505 estimates and 50 fields. Moreover, we have to collect the accumulated estimates given at PDO approval year, and exclude the other updated accumulated estimates that are given after PDO approved year. This provides us with 1072 accumulated estimates and 40 fields, where 345, 364, 363, are for P10, base and P90, respectively. The next step in the filtration process is to remove the estimates which are inconsistent. Additionally, some of the fields and its associated estimates will be removed, if these are not selling gas. Estimates are inconsistent if at least one of these cases occur:

- A field must have three estimates, i.e. P10, mean, and P90 for a specific year to be considered as consistent. If not, the fields and its associated estimates are inconsistent, and cannot be included in our analysis.

- The three accumulated estimates, i.e. P10, mean, and P19, for a field at a specific year have to be unique and in ascending order. If not, the fields and its associated estimates are inconsistent, and cannot be included in our analysis.

After filtering the dataset according to these conditions, we will have 801 estimates and 36 unique fields. Since we have 36 unique fields with unique estimates in ascending order for P10, mean, and P90, the next step is to compare these to the actual saleable gas, which will be elaborated more in the next section, 4.2. Tab. 4.1 shows the entire filtration process of the raw RNB dataset. Note that, data points for saleable oil are neglected since we are only working with saleable gas in this thesis.

Tab. 4.1.: Filtration process for the RNB dataset

Dataset	Number of data points	Number of fields
Original dataset	292 852	113
Dataset with saleable gas	100 553	105
Accumulated estimates	59 802	98
Accumulated estimates since year 2000	13 505	50
Accumulated estimates given at PDO approval year	1042	40
Consistent accumulated estimates	801	36

4.1.2 Data for actual saleable gas

An additional dataset with the information on actual production for both oil and gas, as well as saleable oil and actual saleable gas at field level can be downloaded from `https://factpages.npd.no/en/field/TableView/Production/Saleable/Yearly`. The dataset contains information about the sales volume(oil and gas) for 117 fields, from early 1970´s to 2020. The consistent accumulated saleable estimates for gas, from the bottom of Tab. 4.1 will in the coming sections be compared to actual accumulated saleable gas. Note that, the number of fields are now 36, and have been reduced drastically after excluding the inconsistent estimates from the original dataset, which can be seen from Tab. 4.1. For that reason, the 117 fields from the dataset with actual saleable gas has to reduced to 36 fields as well for us to do the comparison and any analysis further.

4.2 Comparison of saleable gas with estimates

The 36 fields and its associated estimates will be compared to the same fields and its associated actual saleable gas in this section. Two methods are utilised to do the analysis. With the first approach, the actual saleable gas is compared to saleable gas estimates after normalising the data to estimated sale start. The development schedule delay is not considered with this approach. With the second approach, the saleable gas estimates are compared to saleable gas after time shifting the data to actual sale start. With this approach, the development schedule delay is considered. These two methods will be elaborated more in the coming sections.

4.2.1 Normalising saleable data to estimated sale start

Data for estimated sale start of saleable gas will be the basis, as the actual saleable gas will be compared to estimates after estimated sale start. For instance, a field is expected to start sale in year 2000 according to PDO, but due to delay in the development phase of a field, the sale will rather start in year 2001. In this case, the actual saleable gas will be compared to the saleable estimates for year 2000. Note that, the saleable estimates for year 2000 will be compared to a non-existent saleable gas for year 2000, and thus compared to zero. This method addresses the consequences of schedule overruns in production shortfalls (Mohus, 2018). Fig. 4.1 illustrates an example of this case for field, X, on the NCS.

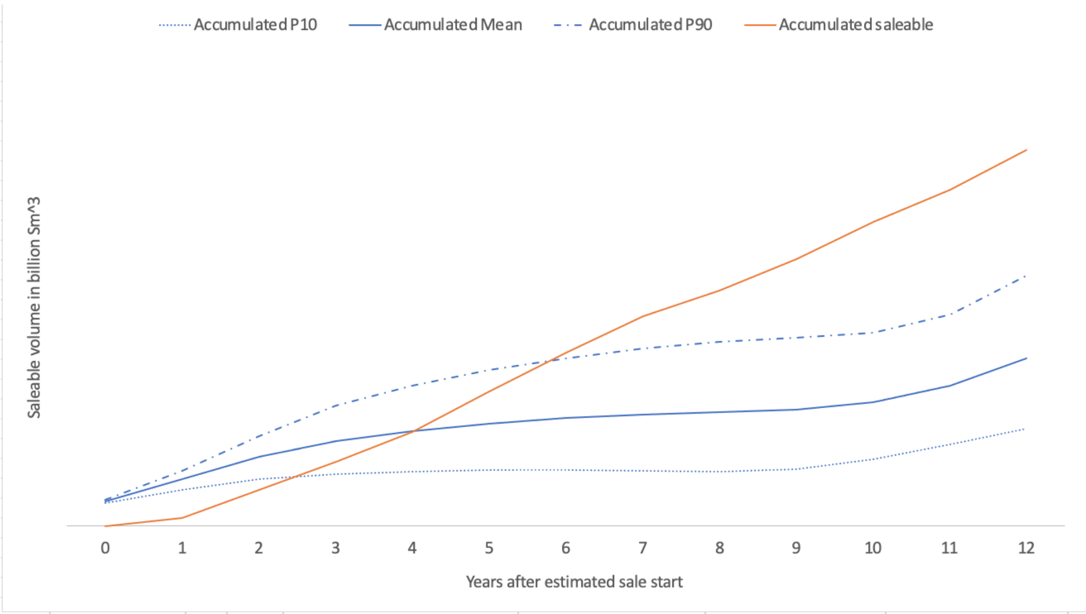

Fig. 4.1.: Field X after normalizing actual saleable gas to estimated sale start

Unbiased forecasts require that 80% of the fields should lie between the constructed P10:P90 interval. For P10, an unbiased forecast contains 10% of fields, which are less or equal to P10. For P90, unbiased forecast contains 10% of the fields, which are higher or equal to P90. By looking at Fig. 4.1, we see that the saleable gas(orange line) is below P10 for the F2Y after estimated sale start. The saleable gas is above P90 from F6Y to F12Y after estimated sale start. Moreover, the saleable gas is higher than mean from F5Y to F12Y estimated sale start. Finally, the saleable gas is between the confidence interval, P10:P90, for the F3Y to F5Y after estimated sale start. Ideally, the field should have been in the constructed P10:P90 interval 80% of the time. However, we can recognize that this is not the case. This is an example of just one field. Tab. 4.2 shows statistics for all the 36 fields when comparing to unbiased forecasts.

Tab. 4.2.: Industry´s ability to forecast after normalising actual saleable gas to estimated sale start(Ignoring delay)

Percentiles	F0Y	F1Y	F2Y	F3Y	F4Y	F5Y	F6Y	F7Y	F8Y	F9Y	F10Y	F11Y	F12Y	F13Y	Unbiased
[P10:P90]	15%	30%	39%	39%	55%	40%	26%	40%	47%	54%	67%	78%	67%	80%	**80%**
Below P10	85%	65%	57%	46%	32%	40%	57%	45%	29%	15%	8%	11%	17%	20%	**10%**
Above P90	0%	4%	4%	14%	13%	20%	17%	15%	24%	31%	25%	11%	17%	0%	**10%**
Above mean	0%	13%	14%	21%	29%	36%	30%	30%	47%	46%	50%	44%	50%	40%	**50%**

Statistics for all the 36 fields from F0Y to F13Y are summarized in Tab. 4.2. The rightmost column shows characteristic of an unbiased forecast. For instance, for the F3Y after estimated sale start, only 39% of the fields fall between the constructed P10:P90 interval. By summarising the other statistics for F3Y, we see that 46% of the fields are below P10, 14% of the fields are higher than P90, and 21% of the fields are higher than mean. In general, from the table, we see that more fields are inside the constructed P10:P90 confidence interval for years after F0Y after estimated sale start. The same is also for "Below P10" and "Above mean" as more fields are approaching the unbiased range in the long run. However, for "Above P90", it is not easy to conclude whether it is approaching the unbiased range. In Tab. 4.3, an average from F0Y to F13Y is summarized. By looking at that table, we can see that the estimates are far from the unbiased forecasts, except for "Above P90".

Tab. 4.3.: Industry´s ability to forecast after normalising actual saleable gas from estimated sale start to F13Y

Percentiles	F0Y - F13Y	Unbiased
[P10:P90]	43%	**80%**
Below P10	44%	**10%**
Above P90	13%	**10%**
Above mean	28%	**50%**

4.2.2 Time shifting estimate data to actual sale start

Data for actual sale start of saleable gas will be the basis, as the saleable gas estimates will be time shifted to sale start of actual saleable gas. The example from subsection, 4.2.1, can be used here as well. The saleable gas estimates after estimated sale start from 2000, will be compared to saleable gas after actual sale start from 2001. Thus, the saleable gas estimates for year 2000 will be time shifted to year 2001, and will be compared to actual saleable gas for that year(F0Y). In conclusion, the saleable gas estimates are shifted one unit to the right compared with the graph, 4.1. Applying this method reduces the impact of schedule delay in the development phase of a field (Mohus, 2018). A graph of time shifting the saleable gas estimates of field, X, to actual sale start is given below.

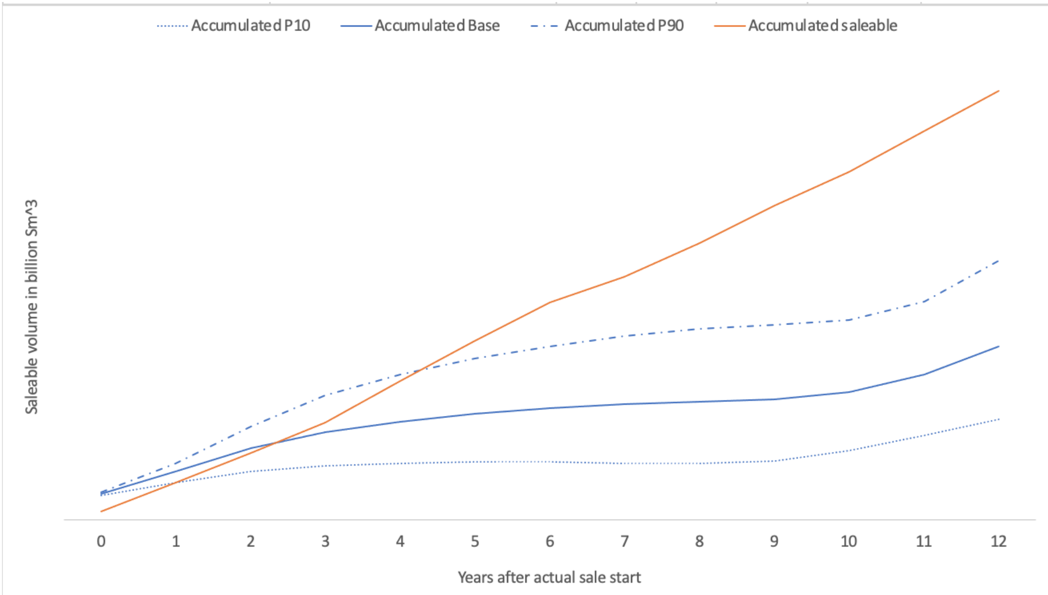

Fig. 4.2.: Overview of the field, X, after time shifting data to actual sale start

The graph illustrates the same field, X, on the NCS. Using the same unbiased characteristics as previously, we see that the saleable gas(orange line) is below P10 from F0Y to F1Y after sale start. From F5Y to F12Y after sale start the saleable gas is above P90. Moreover, the saleable gas is higher than mean from F3Y to F13Y after sale start. Finally, the saleable gas is between the confidence interval, P10:P90, from F2Y to F4Y after sale start. Tab. 4.4 shows statistics for all the 36 fields, when when comparing to unbiased forecasts.

Statistics for all the 36 fields from F0Y to F13Y after sale start are summarized in Tab. 4.4. As before, the rightmost column shows characteristics of unbiased forecasts. Using the F3Y as earlier, we can see that 43% of the fields fall between the constructed P10:P90 confidence interval. By summarising the other statistics for F3Y, we can see that 39% of the fields fall below P10, 18% of the fields are higher than P90, and 32% of the fields are higher than mean. Comparing these statistics to unbiased forecasts in the rightmost column, we can recognize that operators are failing to meet the expectation. From Tab. 4.4, we can see that more fields are nearing the unbiased forecasts as we are approaching the F13Y after actual sale start for "Above mean" and the constructed P10:P90 confidence interval. On the other hand, we cannot conclude that this is the case for "Below P10" and "Above P90", although there are signs for some years, such as F10Y for "Below P10" and F11Y for "Above P90". In Tab. 4.3, an average of F0Y to F13Y is summarized.

Tab. 4.4.: Industry´s ability to forecast after time shifting saleable gas estimates to actual sale start(Considering delay)

Years after sale start	F0Y	F1Y	F2Y	F3Y	F4Y	F5Y	F6Y	F7Y	F8Y	F9Y	F10Y	F11Y	F12Y	F13Y	Unbiased
[P10:P90]	10%	17%	39%	43%	48%	36%	30%	40%	53%	62%	67%	78%	67%	80%	**80%**
Below P10	75%	57%	43%	39%	35%	40%	61%	50%	35%	23%	17%	22%	33%	40%	**10%**
Above P90	15%	26%	14%	18%	16%	24%	17%	15%	18%	23%	25%	11%	17%	0%	**10%**
Above mean	15%	30%	21%	32%	35%	36%	30%	30%	47%	46%	50%	44%	50%	40%	**50%**

Tab. 4.5.: Overview of industry´s ability to forecast after time shifting saleable estimates from actual sale start to F13Y

Years after sale start	F13Y	Unbiased
[P10:P90]	42%	**80%**
Below P10	43%	**10%**
Above P90	18%	**10%**
Above mean	33%	**50%**

By comparing the average from Tab. 4.5 with Tab. 4.3 we can not see any drastic changes. The constructed confidence interval for P10:P90 and "Below P10" are more or less the same. In fact, "Above P90" is a bit worse after time shifting the saleable gas estimates to actual sale start year. On the other hand, "Above mean" is a bit closer to the unbiased forecast with this method, although it is still not good enough.

5 Statistical distribution for the estimates

An essential part of this thesis is to describe the given RNB dataset with the help of a statistical distribution. Therefore, the consistent estimates from Tab. 4.1 will be used in this section to do further analysis. These estimates are fitted to a metalog distribution in order to provide us more information. The statistical tool will help us to generate P50 estimates for all the fields with consistent estimates, by using the P10, mean, and P90 as basis. Additionally, the other percentiles, such as P20, P30, P40, P60, P70 and P80 will also be retrieved with the help of P10, mean, and P90, so that the actual saleable gas can be compared to these percentiles.

5.1 Continuous distribution functions

5.1.1 The metalog distribution

The consistent estimates are analysed through a metalog distribution function. This distribution is more practical to use, as it provides more simplicity and flexibility when the continuous probability functions are unbounded, semibounded, and even bounded. Moreover, the metalog quantile functions and PDFs have simple closed-form expressions that are qunatile parametrized linearly by cumulative-distribution functions (CDFs) (Keelin, 2016). The metalog sheet used in this thesis can be downloaded from the following page `http://www.metalogdistributions.com/home.html`. An Excel file with a metalog sheet gives us the opportunity to assign 10 000 input parameters with a specified probability. Additionally, it is possible to specify the number of terms one wants to utilize in order to develop visual graphs of CDF and PDF. In this thesis, only 3 terms are used for creating metalog distributions, which represent the three estimates, i.e. P10, P50/median, and P90, to get a metalog (MG) mean. Specifically, the P50 input (for which we do not have an actual forecast) is varied in the "metalog" to get a MG mean that matches the forecasted mean. In this thesis, we use the unbounded metalog distribution. This provides us with lower- and upper bounds, which goes from - infinity to + infinity. On the other hand, certain criteria have to be fulfilled to the input parameters to to construct a valid metalog distribution. The following conditions have to be fulfilled for the parameters:

1. The CDF must be monotonically increasing

2. Be defined probabilistically

3. The P50 estimates must lie within the feasible region(A region which gives the P50 a lower- and upper bound)

5.1.2 GRG Nonlinear

Manipulating the P50/median, along with P10 and P90 estimates are vital in order to generate a MG mean. Since we do not have a P50 estimate, we have to go the opposite way. By using the P10, mean, and P90, we can establish a P50 estimate, which provides us a MG mean close to our original mean estimate. To do so, a GRG Nonlinear solving method in Excel is utilised through Solver. This is considered as a potent and reliable approach to work out complicated nonlinear complications over the years. As this is a deterministic method, the GRG solver method requires that defined assumptions are in place to solve the problem. GRG solver presents the absolute value if the relative change of the objective function is lower than the value of tolerance for the last five iterations (Barati, 2013). We used the Excel GRG implementation to find the P50 values that resulted in a metalog distribution with a mean that matched the original mean estimates. An optimal solution can be generated through some specified constraints. Another advantage with this method is the relative speed used to find an optimal answer. For instance, compared to the Evolutionary solver add-in in Excel, the GRG setup requires significantly less time to process the data and to generate our objectives.

5.2 Fitting the estimates to metalog distribution

The consistent accumulated estimates, i.e. P10, mean, and P90, from Tab. 4.1, are fitted in the metalog distribution. In this section we want to see how many of the fields can be fitted in to a metalog distribution by adjusting the relative mean error of a MG mean compared to the original mean. This procedure is done by fitting the estimates to the metalog spreadsheet, which was elaborated in section 5.1. A metalog distribution can only be constructed if the consistent estimates meet the criterion presented in section 5.1.1. When manipulating the median/P50 with the help of GRG Nonlinear solving tool in Excel through Solver, in our case the, MG mean were not 100% equal to the original mean. However, they could be identical given the precision of Excel which has 16 digits. They will certainly be identical if the distributions are symmetric. So the aim is to minimize the relative mean error for all the consistent estimates. To do so, by specifying the constraints in Solver, one can minimize the relative mean error between MG mean and our original mean at hand, given that median/P50 for the different fields are in the feasible region. Equation 5.2 is used to determine how well the MG mean is compared to the original mean.

$$\textbf{Relative mean error} = \frac{\textit{Base mean} - \textit{Metalog mean}}{\textit{Base mean}} \tag{5.1}$$

To minimize the relative mean error, the GRG Nonlinear solving tool in Solver is utilised. Below two screenshots can be seen, Fig. 5.1 and Fig. 5.2. Note that, the values given in Fig. 5.1 are random, and do not show the actual estimates of any fields delivered by the operators, as the intention is just to illustrate how a "3-term" metalog spreadsheet works. The first figure, 5.1, shows a "3-term" metalog spreadsheet, where cells, G28, H28 and I28 represent P10, base/mean, and P90, respectively. Cells G22 and I22 do also represent represent P10 and P90 estimates, respectively, except that cell H22 represents the P50/median, which is the changing variable cell. Note that, is states *median* for cell H22 by default settings in the metalog spreadsheet. These are the input values needed to construct a MG mean in cell D27, which should be close to the target mean(original mean) in cell D28. In cell D29, the relative mean error can be seen. It should be noted that in cells G25 and I25, the feasible range of values for P50 estimate are constructed. This means P50 estimate has to lie within these two values, if not, the third criterion from subsection 5.1.1 is not fulfilled, and thus, the "3-term" metalog spreadsheet cannot provide any values for P50, MG mean, and relative mean error.

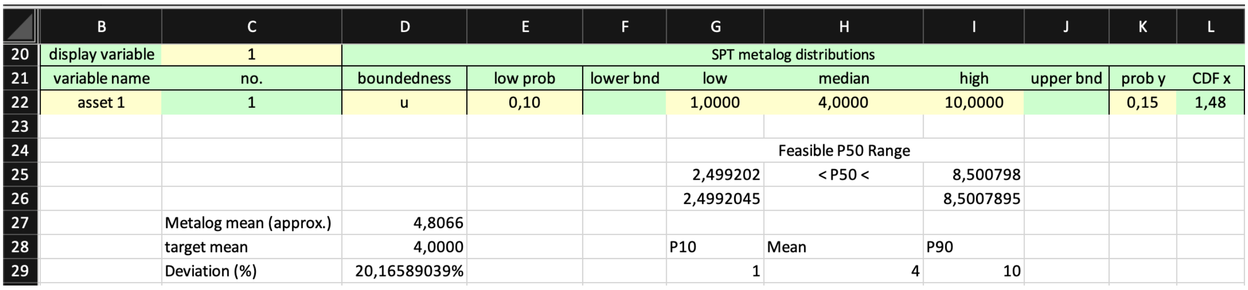

	B	C	D	E	F	G	H	I	J	K	L
20	display variable	1	SPT metalog distributions								
21	variable name	no.	boundedness	low prob	lower bnd	low	median	high	upper bnd	prob y	CDF x
22	asset 1	1	u	0,10		1,0000	4,0000	10,0000		0,15	1,48
23											
24							Feasible P50 Range				
25						2,499202	< P50 <	8,500798			
26						2,4992045		8,5007895			
27		Metalog mean (approx.)	4,8066								
28		target mean	4,0000			P10	Mean	P90			
29		Deviation (%)	20,16589039%			1	4	10			

Fig. 5.1.: Spreadsheet for a metalog distribution before Solver was run

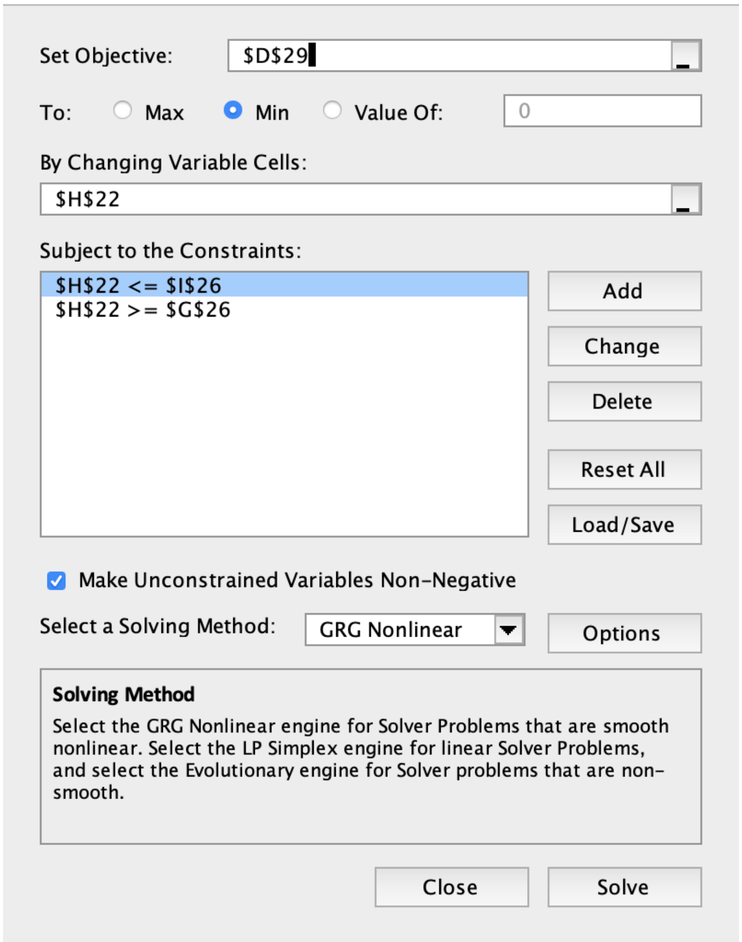

Fig. 5.2.: The specified constraints

Cell D29 from Fig. 5.1, describes the relative mean error, which is set as our objective function in Fig. 5.2. To minimize the error, the following constraints in Fig. 5.2 are specified in Solver to provide a MG mean which is as close as possible to our original mean at hand. As specified in Fig. 5.2, the P50/median from cell H22 in Fig. 5.1, has to lie between values in cells G25 and I25. Fig. 5.3 shows a metalog spreadsheet after the Solver was run can be seen. The median/P50 is adjusted so that the MG mean(cell D27) is close to our target mean(cell D28). Additionally, the relative mean error is reduced to approximately 2,82% in cell D29.

	B	C	D	E	F	G	H	I	J	K	L
20	display variable	1	SPT metalog distributions								
21	variable name	no.	boundedness	low prob	lower bnd	low	median	high	upper bnd	prob y	CDF x
22	asset 1	1	u	0,10		1,0000	2,4992	10,0000		0,15	1,02
23											
24							Feasible P50 Range				
25						2,499202	< P50 <	8,500798			
26						2,4992045		8,5007895			
27		Metalog mean (approx.)	4,1129								
28		target mean	4,0000			P10	Mean	P90			
29		Deviation (%)	2,82258791%			1	4	10			

Fig. 5.3.: Spreadsheet for a metalog distribution after Solver was run

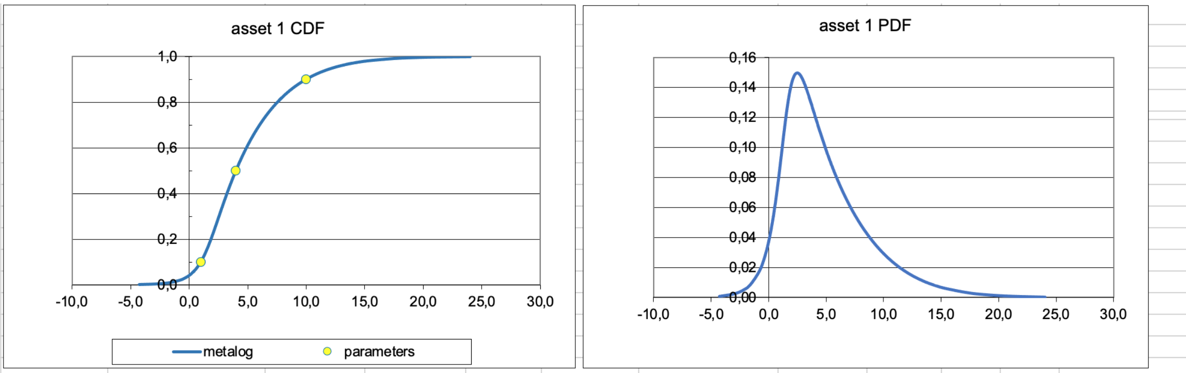

display variable	1	SPT metalog distributions									
variable name	no.	boundedness	low prob	lower bnd	low	median	high	upper bnd	prob y	CDF x	message
asset 1	1	u	0,10		1,0000	4,0000	10,0000		0,15	1,48	

Fig. 5.4.: Prior to Solver was run

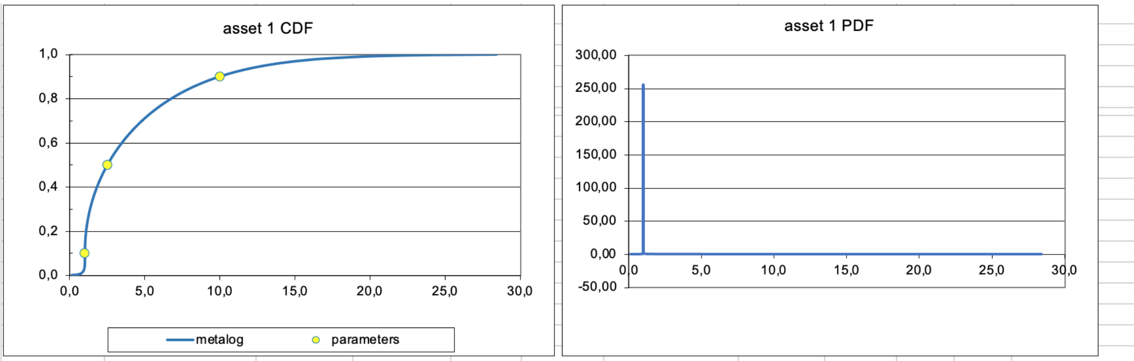

display variable	1	SPT metalog distributions									
variable name	no.	boundedness	low prob	lower bnd	low	median	high	upper bnd	prob y	CDF x	message
asset 1	1	u	0,10		1,0000	2,4992	10,0000		0,15	1,02	

Fig. 5.5.: After Solver was run

Fig. 5.4 reflects a CDF and a PDF prior to Solver was run. Ideally, we would like the MG mean from 5.3 in cell D27 to be equal to target mean(original mean) in D28. However, this is not possible to achieve because of the specific conditions on this type of statistical distribution. Therefore, the MG mean for the different fields will vary a lot, compared to the target mean at hand. This is dependent on the interval of P10, P50, and P90. If the ratio of P10 compared to P50 and P90 is very small, then we would get a higher relative mean error. On the other hand, if the relative ratio of P10 is higher compared to P50 and P90, then the relative mean error will be smaller after it is solved. Fig. 5.5 shows a CDF and PDF after the Solver is run. Doing a similar computation with all the consistent estimates for the different fields result in Tab. 5.1, which shows the number of fields in relation to several adjusted relative mean error.

Tab. 5.1.: Nnumber of fields from F0Y to F13Y for adjusted relative error

Number of fields														
RE	F0Y	F1Y	F2Y	F3Y	F4Y	F5Y	F6Y	F7Y	FY8	F9Y	F10Y	F11Y	F12Y	F13Y	podp
1%	13	15	21	21	23	23	19	15	13	10	10	9	6	5	203
2%	13	16	21	22	28	23	20	18	15	12	11	9	6	5	219
3%	13	17	21	22	28	24	21	18	15	12	11	9	6	5	222
4%	14	19	24	23	28	24	21	19	15	12	12	9	6	5	231
5%	15	19	26	23	28	25	22	19	15	12	12	9	6	5	236
6%	16	19	26	24	28	25	22	19	16	13	12	9	6	5	240
7%	18	20	26	24	30	25	22	19	16	13	12	9	6	5	245
8%	18	20	26	26	31	25	22	19	16	13	12	9	6	5	248
9%	19	21	26	26	31	25	22	19	17	13	12	9	6	5	251
10%	19	21	26	26	31	25	22	20	17	13	12	9	6	5	252
U	20	23	28	28	31	25	23	20	17	13	12	9	6	5	260

Tab. 5.1 illustrates the number of metalog consistent fields. As it can be seen, the number of fields from F0Y to F13Y will increase if we choose to accept a higher relative mean error. At the top of right corner, the podp stands for *pair of data points*. Since the forecast performance for a field is based on the three estimates, we recall that as one podp. In order to provide a statistical interpretation of the fields with the data at hand, we treat P10, mean, and P90 as a pair of three estimates. Thus, one *podp* will consist of one P10, one mean, and one P90, which equals to one field. We can see that the number of metalog consistent fields are largest for the F4Y compared to other years. On the other hand, the number of metalog consistent fields are smallest for the F13Y. The aim is to work with as much fields as possible, and at the same time have a low acceptable margin of relative mean error. For that reason, a 5% relative mean error is chosen, as the *podp* is reduced by 24 compared to U, which consists of 260 *podp*. By choosing *podp* at 5% relative mean error, we have enough data to express these in terms of statistical significance.

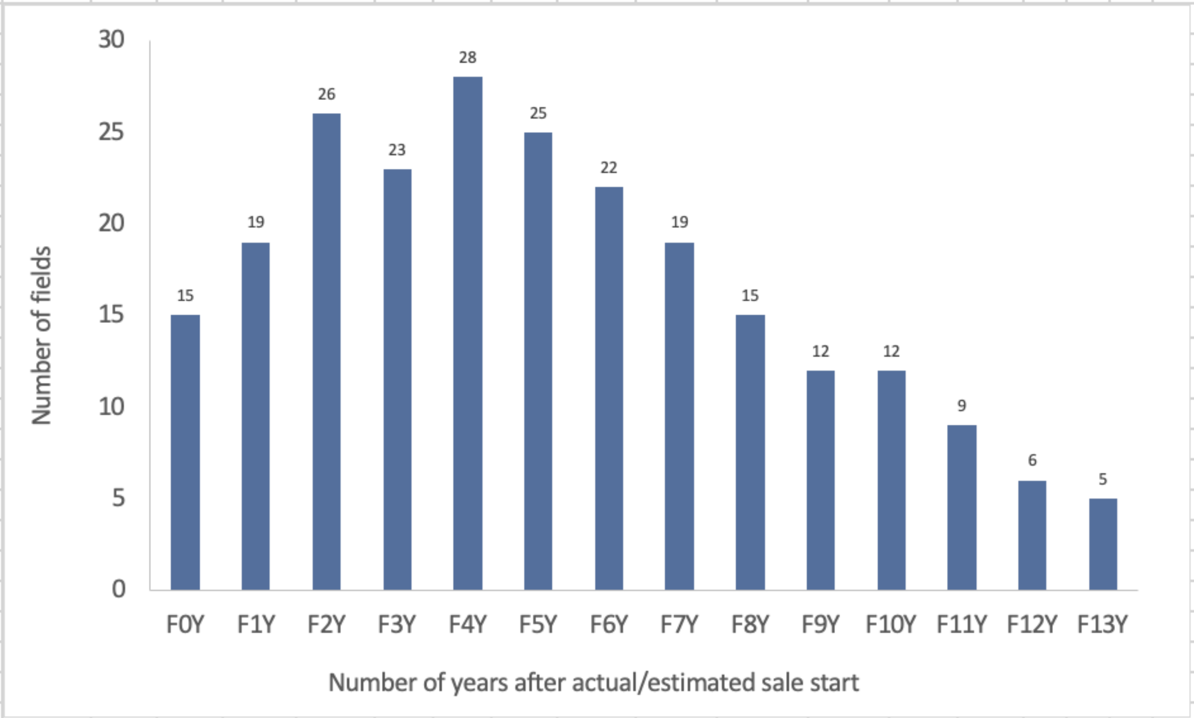

Fig. 5.6.: Number of fields with 5% relative mean error from F0Y and F13Y

In Fig. 5.6, the number of metalog consistent fields for different years are plotted against a 5% relative mean error. The figure can also be used as a basis for evaluating the performance of the forecasters with the actual saleable gas. It must also be taken into account that the varying number of fields for different years will affect the results.

5.2.1 Comparison of the results

Tab. 5.2.: Industry´s ability to forecast after normalising saleable gas to estimated sale start from F0Y to F13Y

Percentage of fields																
	F0Y	F1Y	F2Y	F3Y	F4Y	F5Y	F6Y	F7Y	FY8	F9Y	F10Y	F11Y	F12Y	F13Y	Average	Unbiased
P10:P90	20%	26%	38%	39%	54%	40%	27%	42%	53%	58%	67%	78%	67%	80%	44%	80%
Below P10	80%	68%	58%	52%	36%	40%	55%	42%	27%	17%	8%	11%	17%	20%	43%	10%
Above P90	0%	5%	4%	9%	11%	20%	18%	16%	20%	25%	25%	11%	17%	0%	13%	10 %
Above P50	7%	16%	12%	17%	25%	32%	32%	32%	47%	50%	58%	33%	33%	40%	28%	50%

Tab. 5.3.: Industry´s ability to forecast after normalising saleable gas to actual sale start from F0Y to F13Y

Percentage of fields																
	F0Y	F1Y	F2Y	F3Y	F4Y	F5Y	F6Y	F7Y	FY8	F9Y	F10Y	F11Y	F12Y	F13Y	Average	Unbiased
P10:P90	13%	16%	38%	43%	50%	36%	32%	42%	60%	67%	67%	78%	67%	80%	44%	80%
Below P10	73%	63%	46%	48%	39%	40%	50%	42%	27%	17%	8%	11%	17%	20%	43%	10%
Above P90	0%	11%	15%	17%	7%	12%	27%	21%	20%	17%	17%	33%	17%	20%	16%	10 %
Above P50	20%	26%	23%	22%	25%	32%	32%	32%	47%	50%	58%	33%	33%	40%	31%	50%

The number of fields from Fig. 5.6 for F0Y to F13Y provide us Tab. 5.2 and Tab. 5.3 when comparing them to the unbiased forecasts. On the rightmost column we the unbiased forecasts. Tab. 5.2 shows the percentage of fields when compared to estimated sale start. On the other hand, Tab. 5.3 shows the percentage of fields when compared to actual sale start. By comparing the two tables, we cannot see any significant difference between them. From the constructed P10:P90 confidence interval, we see that the percentage of fields lying in that range are the same for both tables. It should be noted that the results for P10:P90, "below P10", and "Above P90" are the same, as it was in Tab. 4.2 and in Tab. 4.4, with some small changes in different years. The main reason for that is because we have excluded some fields after we choosing to work with fields at a 5% relative mean error. The average for the constructed P10:P90 from F0Y to F13Y does also indicate that in Tab. 5.2 and Tab. 5.3. The same can also be said for "Below P10". For "Above P90", we can see there is a marginal difference between the tables from F0Y to F13Y. Actually, when comparing the saleable gas estimates to the actual sale start, the result is a bit worse. The average of 13% from Tab. 5.2 has increased to 16% in Tab. 5.3. On the other hand, the generated P50 from the previous chapter is utilised in both tables. According to Tab. 5.2 and Tab. 5.3, on average, the generated P50 are 28% and 31%, respectively. These are far from the unbiased forecasts for P50. The result is worst for F0Y from both tables. Despite that fact, for some years we can see that the generated P50 are actually close to, or even match the unbiased forecasts for P50, without us being able to conclude whether it is purely coincidental or deliberate.

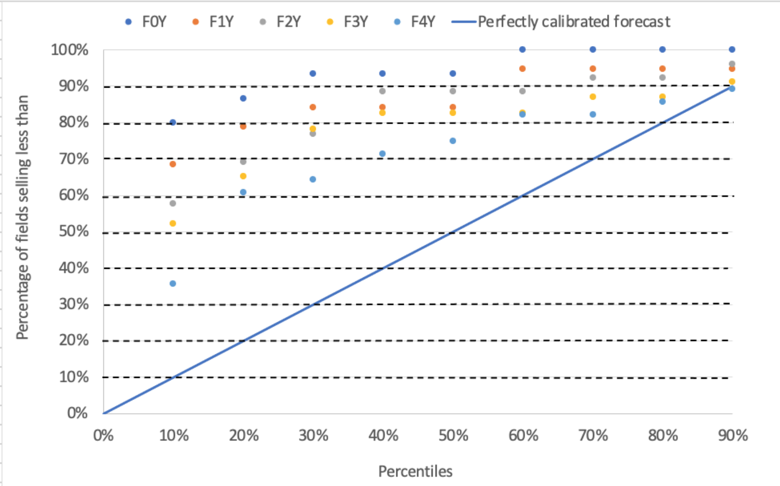

Fig. 5.7.: Sensitivity analysis from F0Y to F4Y compared to estimated sale start

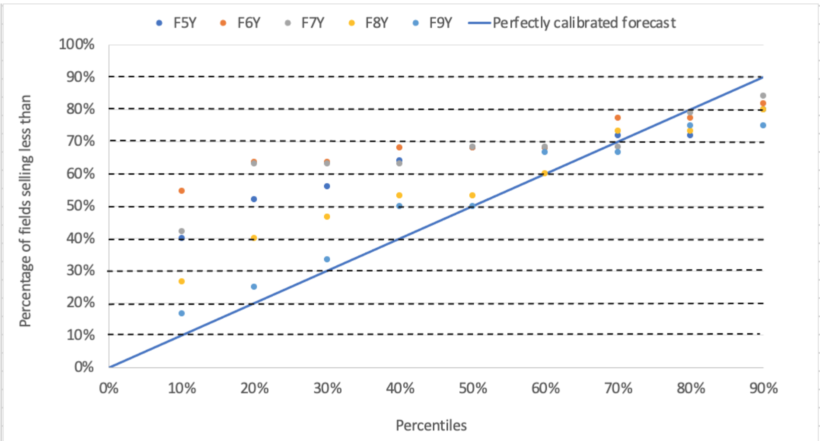

Fig. 5.8.: Sensitivity analysis from F5Y to F9Y compared to estimated sale start

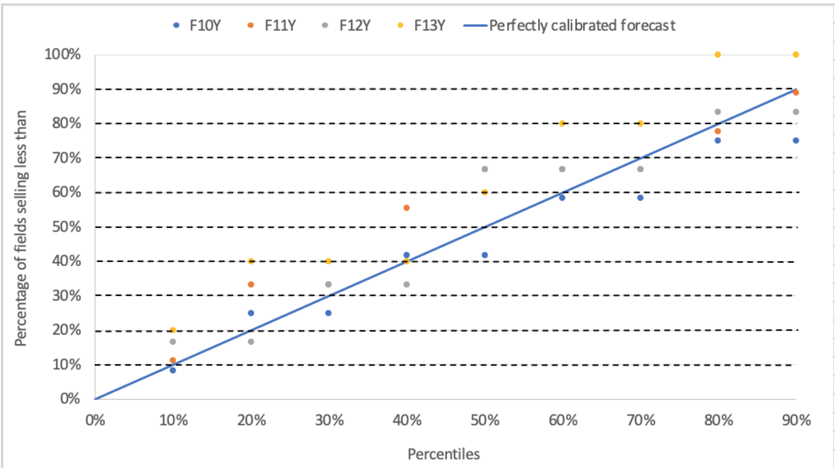

Fig. 5.9.: Sensitivity analysis from F10Y to F13Y compared to estimated sale start

Using the other percentiles, as mentioned in section 5, will give us more insight about the saleable gas estimates compared to the unbiased characteristics. Fig. 5.7, Fig. 5.8, and Fig. 5.9 present a sensitivity analysis when the data for actual saleable gas is normalized to estimated sale start. The first figure shows the sensitivity analysis done for F0Y to F4Y, the second figure shows for F5Y to F9Y, and the third figure shows for F9Y to F13Y. The percentiles are on the X-axis, while the Y-axis shows the percentage of fields whose accumulated saleable gas does not exceed the accumulated forecasts for saleable gas. The colored dots in all figures represent the percentage of fields for different years compared to percentiles from P10 to P90. Fig. 5.7 illustrate that percentiles are not close to the perfectly calibrated forecast(blue diagonal line). But still, we see that the percentage of fields are showing some improvement for F4Y. In Fig. 5.8, we can see some improvement compared to the previous figure. For F9Y we can recognize that the percentage of fields are nearing the diagonal line. However, the percentage of fields are still away from the unbiased forecasts. In Fig. 5.9, we can see that even more fields are nearing, and even touching the unbiased forecast. For instance, for F10Y(blue dots), F11Y(orange dots), F12Y(grey dots), and F13Y(yellow dots) we can see improvement compared to the two previous figures. Among these, especially for F13Y, we see that the yellow dots are a bit far away from the unbiased forecast. A similar analysis is also done for saleable gas estimates when they are time shifted to actual sale start. The results are very similar. For that reason, the graphs can be seen in Appendix B.

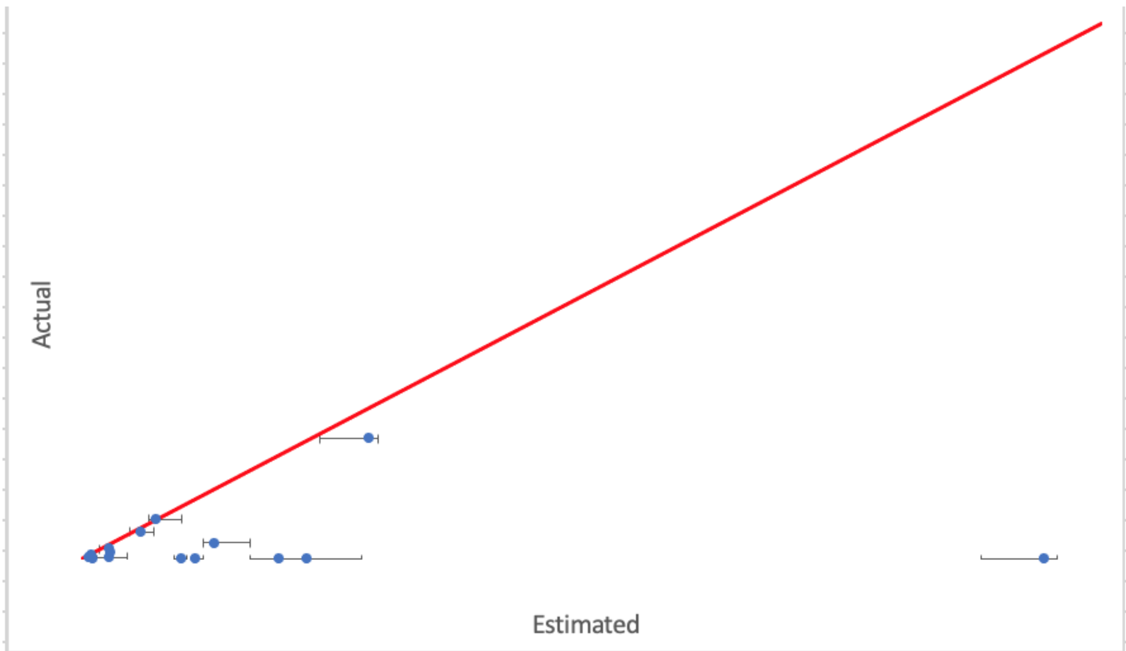

Fig. 5.10.: Without delay: Scatterplot for all fields for F0Y

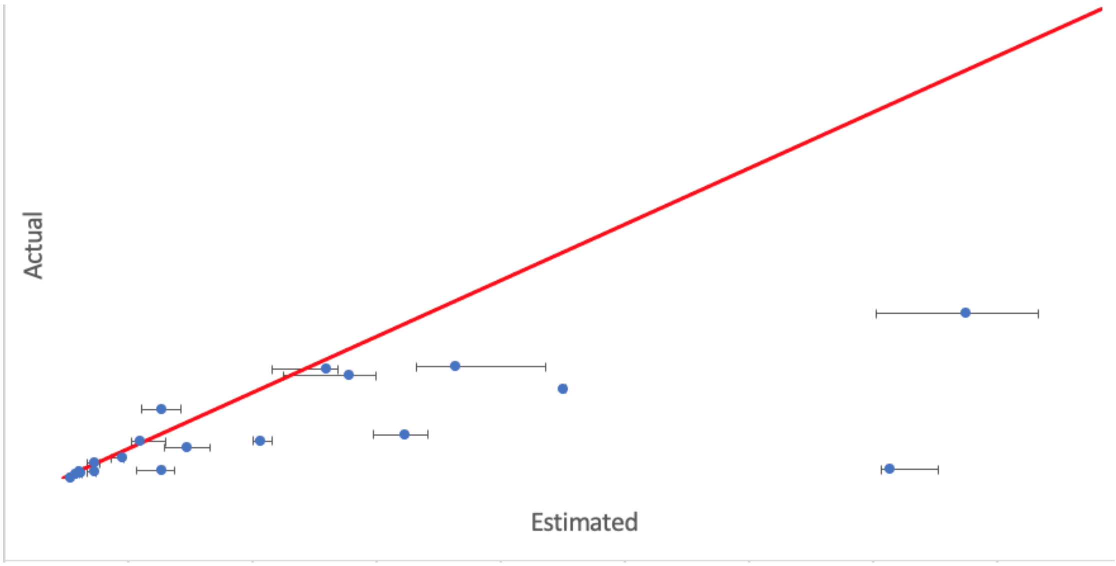

Fig. 5.11.: Without delay: Scatterplot for all fields for F1Y

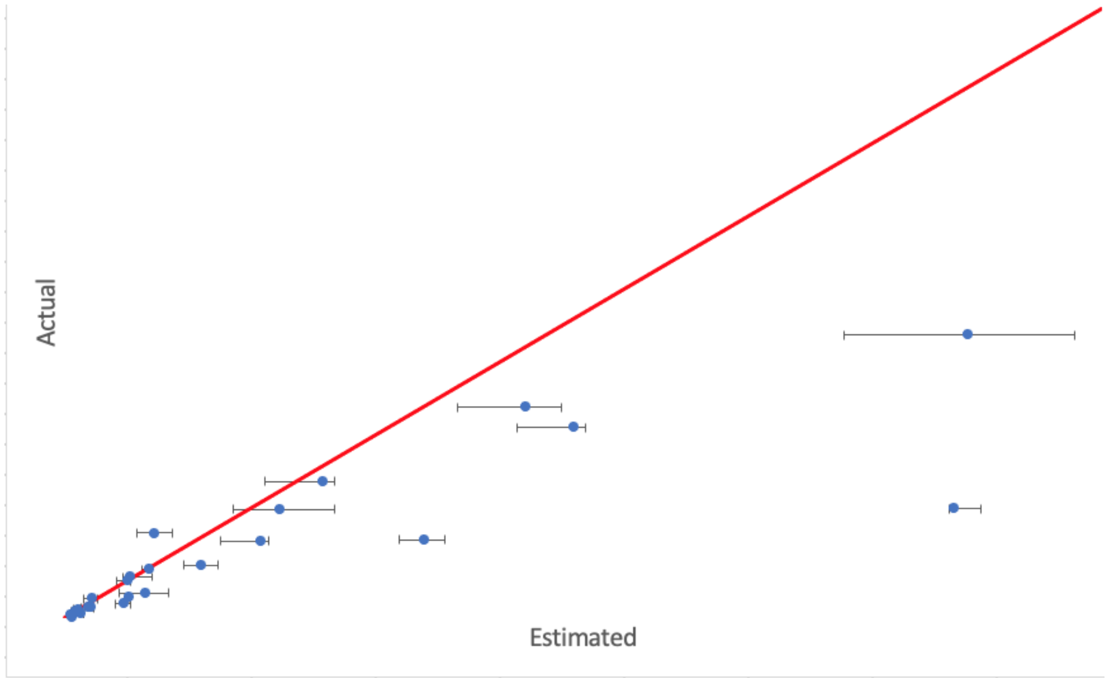

Fig. 5.12.: Without delay: Scatterplot for all fields for F2Y

By looking at the scatter plots for F0Y, F1Y, and F2Y we can be sure that there is overconfidence, optimism, and pessimism among the operators. In Fig. 5.10 there are 15 fields, only 3 fields(20%) touched the 45-degree line, which indicate overconfidence. On the other hand, 1 field(6,7%) fell above the 45-degree line, while 14(93,3%) fields fell below the 45-degree line, which indicates both pessimism and and optimism, respectively

In Fig. 5.11 there are 19 fields. Among these, only 5 fields(26,3%) touched the 45-degree line, which indicates overconfidence. Additionally, only 3 fields(15,8%) fell above the

45-degree line, while the other 14 fields(84,2%) fell below the 45-degree line, which indicates both pessimism and optimism, respectively.

In Fig. 5.12 there are 26 fields. Among these, 10 fields(38,5%) touched the 45-degree line, which indicates overconfidence. Additionally, only 3 fields(11,5%) fell above the 45 degree-line, while the other 23 fields(88,5%) fell below the 45-degree line, which indicates both pessimism and optimism, respectively.

In the appendix D, the remaining graphs from F3Y to F13Y can be seen. From those graphs, we can see that the number of percentiles touching the 45-degree is increasing as the more and more years pass.

5.3 Scatter plots; Comparing P10, P50, and P90 with saleable gas when delay is considered

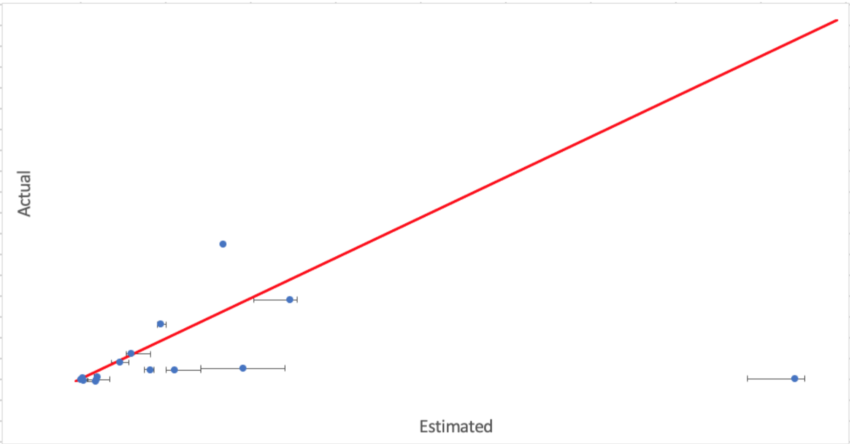

Fig. 5.13.: With delay: Scatter plot for all fields for F0Y

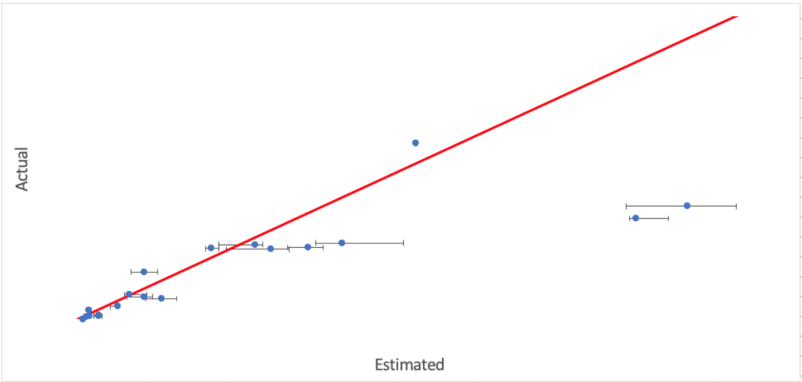

Fig. 5.14.: With delay: Scatter plot for all fields for F1Y

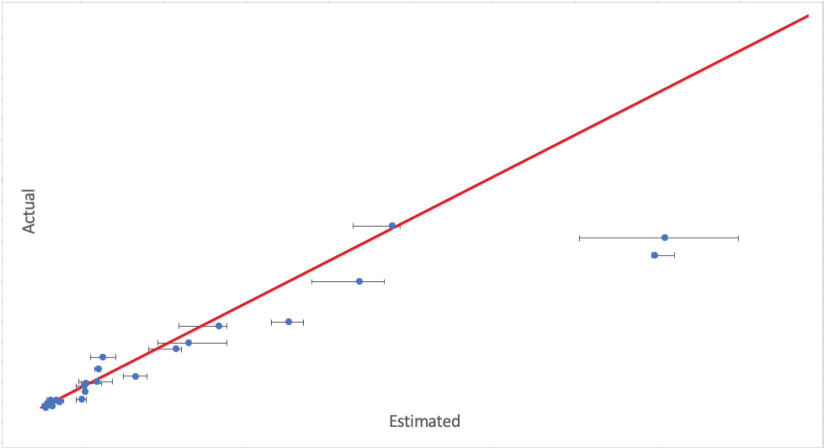

Fig. 5.15.: With delay: Scatter plot for all fields for F2Y

By looking at the scatter plots for F0Y, F1Y, and F2Y we can be sure that there is overconfidence, optimism, and pessimism among the operators. From Fig. 5.13, only 2 fields(13,33%) touched the 45-degree line, which indicate overconfidence. On the other hand, 2 fields fell above the 45-degree line, while 13 fields fell below the 45-degree line, which indicates both pessimism and and optimism, respectively

In Fig. 5.14 there are 19 fields. Among these only 3 fields(15,8%) touched the 45-degree line, which indicates overconfidence. Additionally, only 5 fields(26,3%) fell above the 45-degree line, while the other 14 fields(73,7%) fell below the 45-degree line, which indicates both pessimism and optimism, respectively.

In Fig. 5.15 there are 26 fields. Among these, 10 fields(38,5%) touched the 45-degree line, which indicates overconfidence. Additionally, only 6 fields(23,1%) fell above the 45 degree-line, while the other 20 fields(76,92%) fell below the 45-degree line, which indicates both pessimism and optimism, respectively.

In the appendix E, the remaining graphs from F3Y to F13Y can be seen. From those graphs, we can see that the number of percentiles touching the 45-degree is increasing as the more and more years pass.

Discussion 6

6.1 Filtration of estimates

6.1.1 Limited data for saleable gas estimates

The consistent saleable gas estimates at hand were very limited. There are many reasons for that; 1. The operators forecast were the same for some of the, or for all the P10, mean, and P90 for a specific field(s) for a given year. As a result of that, a significant number of forecasts had to be reduced for a field. Thus, the podp used for the analysis in the thesis, were less than what one ideally would have had. Having a similar scenario for all the fields do have a significant effect, when analysing the saleable gas estimates according to a well-calibrated forecast. Due to limited saleable gas estimates for a particular year after estimated/actual sale start, the results could be misleading. Originally, there were saleable gas estimates for the F17Y after estimated/actual sale start. However, due to few *podp*, such as 3 *podp* for F14Y, 2 *podp* for F15Y, 1 for *podp* F16Y, and 1 for *podp* F17Y, these had to be neglected, as these were too few in order to include in the analysis.

The second issue appears, when certain fields are not selling any gas at all compared to operator´s forcasted estimates. Because of that, 4 fields were excluded. This can also be seen at the 2 last rows from Tab. 4.1.

The third issue appears, when we do not have data for saleable gas estimates for a particular year after estimated sale start due to inconsistency. This could potentially lead to a misleading result for an arbitrary year after estimated sale start. For instance, let us say a the forecast is delivered for the F10Y after estimated sale start, for a field. But due to either missing, or inconsistency in estimates, we can only use estimates from F7Y to F10Y after estimated sale start.

From year 2000 to year 2020, 62 fields got PDO approval according to the reports from NPD. Similarly, focusing on the same time period from the RNB dataset for the saleable gas estimates, provides us 36 unique fields. Below, two tables are shown. Tab. 6.1 shows the dataset collected from the NPD´s website, and highlights the number of fields we would have liked to work with. Tab. 6.2 highlights the 36 fields at the bottom, we had to work with.

Tab. 6.1.: Overview of number of fields for the entire period from original dataset vs number of fields after PDO approval from year 2000 and onwards

Dataset from NPD	Number of unique fields
Original	117
PDO approval from year 2000 and onwards	**62**

Tab. 6.2.: Overview of the filtration process for the RNB dataset

RNB Dataset	Number of datapoints	Number of unique fields
Original dataset	292 852	113
Dataset with saleable gas	100 553	105
Accumulated estimates	59 802	98
Accumulated estimates as of year 2000 and further	13 505	50
Accumulated estimates given at PDO approval year	1042	40
Consistent accumulated estimates	801	**36**

6.1.2 Removing the delay

Many of the fields on NCS had schedule delays regarding their production start. A delay in production start, does also lead to a delay in sale start. The saleable gas estimates after estimated sale start were compared to its respective years for saleable gas, as elaborated in section 4.2.1. In this case, the estimates for saleable gas were compared to zero until the first sale of gas started. However, this approach does not take into account for the schedule delays. With the intention of eliminating the schedule delays, the estimates for saleable gas were time shifted to actual sale start for all the fields, as explained in section 4.2.2. Doing so, gave us a "better" interpretation of the fields regard to perfectly calibrated forecasts, although it did not improve the results significantly. Additionally, applying this approach reduced the effects of scheduled delays to some extent, although eliminating them completely are unreasonable without more detailed data. After time shifting the saleable gas estimates to actual sale start, we were left with 34 fields at 5% relative mean error.

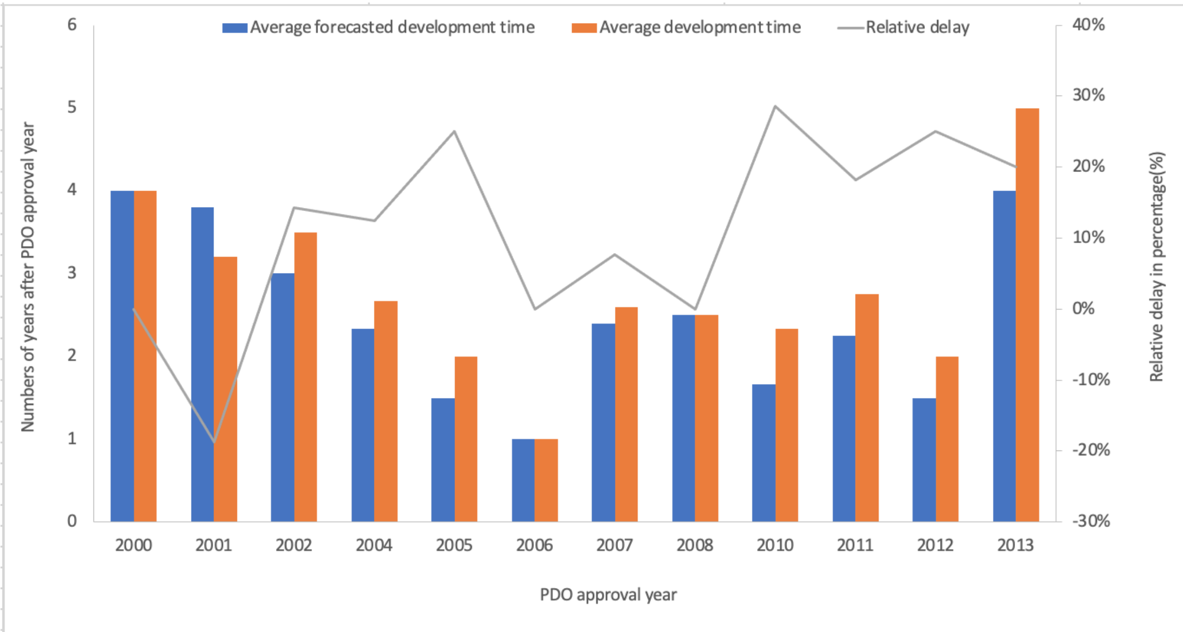

Fig. 6.1.: Comparison of forecasted development time and average development time given at PDO approval year

Fig. 6.1 above shows a graph for fields that got PDO approval year, when using the data at 5% relative mean error from Tab. 5.6. The average forecasted development time and the average development time, compared to PDO approval year, on is the X-axis. The Y-axis shows the number of year after PDO approval year. The grey line indicates the relative delay between the average forecasted development time and the average development time. From the graph, we see that the average development time exceeds the average forecasted development time for 8/12 PDO approval years. In year

2000, 2006, and 2008, the average forecasted development time matched the average forecasted time. On the other hand, in year 2001, the average forecasted development time exceeded the average development time.

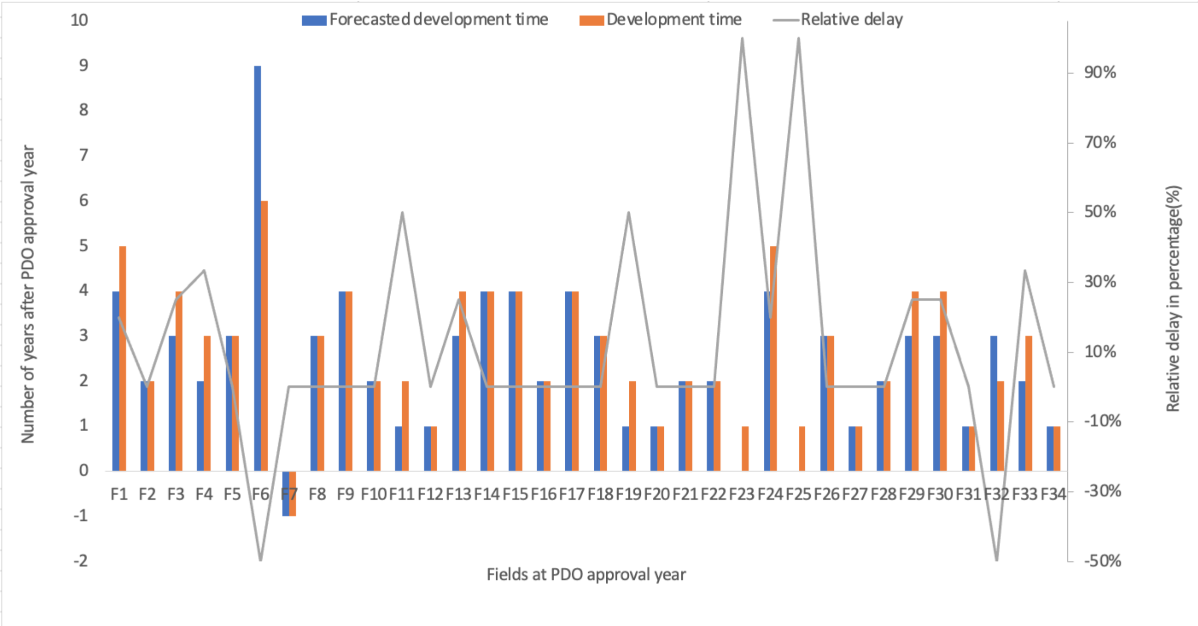

Fig. 6.2.: Comparison of forecasted development time and the development at field level, given at PDO approval year

If we go even deeper, Fig. 6.2, shows the forecasted development time and the development time for all the fields, given at PDO approval year. On the X-axis we see the number of fields from its PDO approval year, while the y-axis shows the number of year from PDO approval year. The grey line indicates the relative delay in terms of percentage between the forecasted development time and the actual development time. There is no way of ensuring that we will be correct at the individual level, but we should be correct at the accumulated field level. Therefore, the forecasted development time should be equal to the actual development time. This is what one ideally wants to achieve. By looking at the graph, for all the fields, we see that 13/34 fields had used more time than what was expected. Among these, For field 23 and field 25, the forecasted development time was set to be at the PDO approval year, however, the development time was actually 1 year after that. 19/34 fields spent as many years they had been forecasted for. On the other hand, for field 7, the both the forecasted development time and actual development time(orange bar) was set one year before PDO approval year. Using the Fig. 6.2 as basis, despite the fact that, a little more than 50% of the fields are using the same development time as forecasted, on the other hand, a bit less than 50% of fields are not matching the forecasted development time. This is a concerning trend for the future. As Hayashi et al. have discussed the concept of VoI is important taking decision regarding development of fields. This concept is utilised in an economic criterion when making decisions, which includes the quantification of uncertainties and economic assessment numerous reservoir situations. Seeking to add new information, is adequate when eliminating geological uncertainties. Thus, can help help to reduce the cost and the delay in the project implementation.

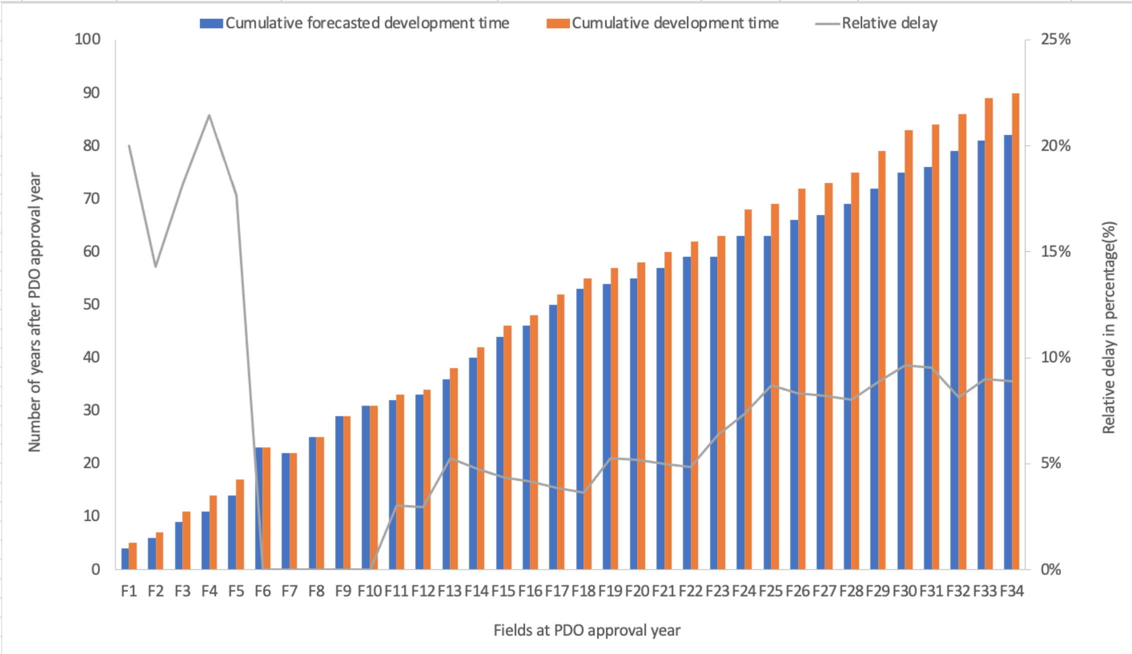

Fig. 6.3.: Cumulative forecasted development time and actual development time for all fields, given at PDO approval year

Fig. 6.3 shows the cumulative forecasted development time and the real cumulative development time(orange bar) by adding up all the 34 fields from PDO approval year when moving to right on the X-axis. The grey line indicates the relative delay between these two, as we are moving to the right on the X-axis

6.1.3 Selection of FnY

In this thesis, we are looking at the fields that got PDO approval from year 2000 to year 2020. Given the consistent estimates for saleable gas, we are only investigating from F0Y to F13Y after estimated/actual sale start. Having said that, we could have investigated for F14Y to F17Y as well. Including them into our analysis would have affected the results. The podp for these years were less, and are not included. The next question to be asked is whether the number of accumulated years (FXY) affects the performance. By looking at Tab. 5.1 for 5% relative mean error wee that the number of fields are changing as we go further to the right on the X-axis. Ideally, we would have liked the number of fields in all these years to be the same in order to get a "better" interpretation of the results. However, for some years we are working with less fields, and for other years, we are working with more fields. The variation in number of fields, will most likely affects the results from the analysis. Adding the sensitivity analysis done, and including Fig. 5.7, Fig. 5.8, and Fig. 5.9 show that as we are approaching the unbiased forecasts from F10Y to F13Y compared to, let´s say, F0Y to F4Y. Thus, the results show that the forecasts are "better" in the long run, i.e. many years after estimated start, rather than the first few years.

6.1.4 Selection of 3-term for metalog distribution

The operators are asked to provide only 3 numbers. The number of terms for a metalog distribution depends on the context and purpose (Keelin, 2016). In this thesis, since we are only given three estimates, i.e. P10, mean, and P90, it is natural to use a 3-term($n=3$). Therefore, in this case, as long as the data is feasible, the metalog CDF will pass through these points perfectly as shown in Fig. 5.4. The input parameters used, such as P10, mean, and P90 must be assigned with a probability. In our case, the mean forecast does not have a probability. Therefore, a feasible P50 is selected with the help of GRG nonlinear tool in Excel.

6.1.5 Selection of acceptable relative mean error

With the choice of an appropriate relative mean error between the MG mean and the original mean(target mean), a 5% relative mean error was chosen from Tab. 5.1. From the table, we clearly see that a higher relative mean error gives us the opportunity to include more fields. However, selecting fields based on high relative mean error, will also make the metalog mean less accurate, as these are based on P10, manipulation of P50, and P90. Therefore, selecting fields based on low error in the relative mean is better for the analysis in this thesis. A very low error is not optimal either, since a significant number of fields have to be removed with 1% relative mean error. The removal of fields is clear from F0Y to F8Y when moving down from U to 1%. At the same time, we see from F9Y to F13Y, the reduction in number of fields are less when going down from U to 1% relative mean error. Thus, choosing a low error in the relative mean at 5% with 236 podp compared to U relative mean error with 260 podp is more acceptable.

7 Conclusion

This thesis presents an analysis of 40 fields that got PDO approvals after FID in year 2000 or later. The operator´s forecasts from F0Y to F13Y when considering without delay(estimated sale start), and with delay(actual sale start), are compared to a well-calibrated forecast. On average, without including the delay, 43% of saleable gas estimates fell between the constructed P10:P90 confidence interval, while 44% were below P10 and 13% were above P90. On the other hand, when considering the delay, after time shifting the data, 42% fell between the constructed P10:P90 confidence interval, while 43% fell below P10, and 18% fell above P90. This reflects the optimism and overconfidence in operator´s forecasts.

Initially, we did not have any P50 from the raw RNB dataset. Instead, we were given a mean estimate. The P50 was important to us, since it expressed uncertainty from NPD. Therefore, a metalog distribution was utilised to capture that, in addition to other percentiles, such as P20, P30, P40, P60, P70 and P80. Since the metalog distribution provided us MG mean with different relative mean error. Thus, an error of 5% relative mean was chosen for the analysis. The P50 without delay showed that on average, 28% of fields were selling gas above P50, while considering the delay, 31% of the fields were selling gas above P50. These results did not fulfill the criteria for an unbiased forecast for P50. In addition, a sensitivity analysis was done without delay, and showed the number of fields for the different percentiles when compared to a perfectly calibrated forecast. From the sensitivity analysis, we see that the results are poor from F0Y to F4Y. However, it improves from F5Y to F9Y. Finally, from F10Y to F13Y, even more fields are approaching the perfectly calibrated forecast. The results from this thesis clearly indicate the biases in the forecasts provided by the operators. Thus, the operators have to improve their forecasts for the fields on the NCS, and should get more attention. This is needed to reduce overconfident and optimism. Main factors psychological factors such as *deception* and *delusion*, which were described in subsections, 3.2.1 and 3.2.3. Finally, for further studies, applying Reference class forecasting (RCF) for improving the saleable gas estimates is an option. This is an endorsed new forecasting method based on theories of planning and decision-making by Daniel Kahneman. This takes into account inaccuracy in terms of optimism bias and strategic misrepresentation (Flyvbjerg, 2008).

References

Aven, T. (2015). Implications of black swans to the foundations and practice of risk assessment and management. *Reliability Engineering & System Safety*, *134*, 83–91.

Barati, R. (2013). Application of excel solver for parameter estimation of the nonlinear muskingum models. *KSCE Journal of Civil Engineering*, *17*(5), 1139–1148.

Bratvold, R. B., Begg, S., & Campbell, J. (2002). Would you know a good decision if you saw one? In *Spe annual technical conference and exhibition.*

Bratvold, R. B., Mohus, E., Petutschnig, D., Bickel, E., et al. (2020). Production forecasting: Optimistic and overconfident—over and over again. *SPE Reservoir Evaluation & Engineering*.

Energies, P. (2015). *The life cycle of oil and gas fields.* `https://www.planete-energies.com/en/medias/close/life-cycle-oil-and-gas-fields`.

Fernando, J. (2021). *Time value of money (tvm).* `https://www.investopedia.com/terms/t/timevalueofmoney.asp`.

Floris, F. J., Bush, M., Cuypers, M., Roggero, F., & Syversveen, A. R. (2001). Methods for quantifying the uncertainty of production forecasts: a comparative study. *Petroleum Geoscience*, *7*(S), S87–S96.

Flyvbjerg, B. (2007). Policy and planning for large-infrastructure projects: problems, causes, cures. *Environment and Planning B: planning and design*, *34*(4), 578–597.

Flyvbjerg, B. (2008). Curbing optimism bias and strategic misrepresentation in planning: Reference class forecasting in practice. *European planning studies*, *16*(1), 3–21.

Flyvbjerg, B., Garbuio, M., & Lovallo, D. (2009). Delusion and deception in large infrastructure projects: two models for explaining and preventing executive disaster. *California management review*, *51*(2), 170–194.

GasWiki. (2021). *Reservoir simulation.* https://en.wikipedia.org/wiki/Reservoir_simulation.

Hayashi, S., Ligero, E., & Schiozer, D. (2010). Risk mitigation in petroleum field development by modular implantation. *Journal of Petroleum Science and Engineering*, *75*(1-2), 105–113.

Keelin, T. W. (2016). The metalog distributions. *Decision Analysis*, *13*(4), 243–277.

Mohus, E. (2018). *Over budget, over time, and reduced revenue, over and over again-an analysis of the norwegian petroleum industry's inability to forecast production* (Unpublished master's thesis). University of Stavanger, Norway.

Nandurdikar, N. S., Wallace, L., et al. (2011). Failure to produce: An investigation of deficiencies in production attainment. In *Spe annual technical conference and exhibition.*

of Petroleum, N. M., & Energy. (2018). Guidelines for plan for development and operation of a petroleum (pdo) and plan for installation and operation of facilities for transport and utilisation of petroleum(pio). *Marine Policy*, *53*, 8, 38.

Petroleum, N. (2020). *Resource classification.* https://www.npd.no/en/regulations/reporting_and_applications/revised-national-budget/3-resource-classification/.

Petroleum, N. (2021a). *Eksport av olje og gass.* https://www.norskpetroleum.no/produksjon-og-eksport/eksport-av-olje-og-gass/.

Petroleum, N. (2021b). *Historisk produksjon.* https://www.norskpetroleum.no/fakta/historisk-produksjon/#arlig.

Petroleum, N. (2021c). *Production forecasts.* https://www.norskpetroleum.no/en/production-and-exports/production-forecasts/.

PetroWiki. (2021). *Uncertainty analysis in creating production forecast.* https://petrowiki.spe.org/Uncertainty_analysis_in_creating_production_forecast.

Siddiqui, M. A., Al-Yateem, K. S., Al-Thawadi, A., et al. (2007). A new tool to evaluate the feasibility of petroleum exploration projects using a combination of deterministic and probabilistic methods. In *Spe middle east oil and gas show and conference*.

Welsh, M. B., Begg, S. H., Bratvold, R. B., et al. (2007). Modelling the economic impact of common biases on oil and gas decisions. In *Spe annual technical conference and exhibition*.

Welsh, M. B., Bratvold, R. B., Begg, S. H., et al. (2005). Cognitive biases in the petroleum industry: Impact and remediation. In *Spe annual technical conference and exhibition*.

Appendix A

A.1 The metalog distribution

The process explained in section 5.2, are utilised to assist our P10, mean, and P90 at hand, and additionally provide us more insights about each field. In our case, a 3-term unbounded metalog distribution was utilised. This section will explain the unbounded metalog distribution, as well as how the PDF´s and CDF´s are retrieved:

Definition 1: The metalog quantile function with n terms: (Keelin, 2016)

$$M_n(y;\mathbf{x},\mathbf{y}) = a_1 + a_2 \ln \frac{y}{1-y} \tag{A.1}$$

for n=2

$$M_n(y;\mathbf{x},\mathbf{y}) = a_1 + a_2 \ln \frac{y}{1-y} + a_3(y-0.5)\ln \frac{y}{1-y} \tag{A.2}$$

for n=3

$$M_n(y;\mathbf{x},\mathbf{y}) = a_1 + a_2 \ln \frac{y}{1-y} + a_3(y-0.5)\ln \frac{y}{1-y} + a_4(y-0.5) \tag{A.3}$$

for n=4

For terms above $n = 4$

$$M_n(y;\mathbf{x},\mathbf{y}) = M_{n-1} + a_n(y-0.5)^{\frac{n-1}{2}} \tag{A.4}$$

for odd $n \geq 5$

$$M_n(y;\mathbf{x},\mathbf{y}) = M_{n-1} + a_n(y-0.5)^{\frac{n}{2}-1}\ln \frac{y}{1-y} \tag{A.5}$$

for odd $n \geq 6$,

The cumulative probability for for y yields from 0 < y < 1. The CDF consists the coordinates for x and y, where $\mathbf{x} = (x_1, \ldots, x_m)$ and $\mathbf{y} = (y_1, \ldots, y_m)$ of length $m >= n$, $0 < y_i < 1$ for each y_i, and at least n of the y_i's are distinct. The column vector of scaling constants $\mathbf{a} = (a_1, \ldots, a_n)$ (Keelin, 2016).

Using A.5 as basis, and differentiating that with respect to y and inverting the results provide the metalog probability density function (PDF) (Keelin, 2016):

$$M_n(y) = \frac{y(1-y)}{a_2} \tag{A.6}$$

for n=2

$$M_n(y) = \frac{(1)}{\frac{a_2}{y(1-y)} + a_3(\frac{y-0.5}{y(1-y)} + \ln\frac{y}{1-y})} \tag{A.7}$$

for n=3

$$M_n(y) = \frac{(1)}{\frac{a_2}{y(1-y)} + a_3(\frac{y-0.5}{y(1-y)} + \ln\frac{y}{1-y}) + a_4} \tag{A.8}$$

for n=4

$$M_n(y) = \left[\frac{1}{m_{n-1}(y)} + a_n\frac{n-1}{2}(y-0.5)^{\frac{n-3}{2}}\right]^{-1} \tag{A.9}$$

for odd $n >= 5$

$$M_n(y) = \left[\frac{1}{m_{n-1}(y)} + a_n\frac{(y-0.5)^{\frac{n}{2}-1}}{y(1-y)} + (\frac{n}{2}-1)(y-0.5)^{\frac{n}{2}-2}\ln\frac{y}{1-y}\right]^{-1} \tag{A.10}$$

for even $n >= 6$

The PDF, $m_n(y)$, is given as a function of cumulative probability *y*. To plot this PDF, with random values of **X** on the horizontal axis, the $M_n(y)$ is used, while adjusting $m_n(y)$ on the vertical axis, and vary *y* ∈ (0,1) to yield the corresponding values on both axes (Keelin, 2016).

Supplementary results

B

B.1 Sensitivity analysis for saleable gas estimates after time shifting to actual sale start year

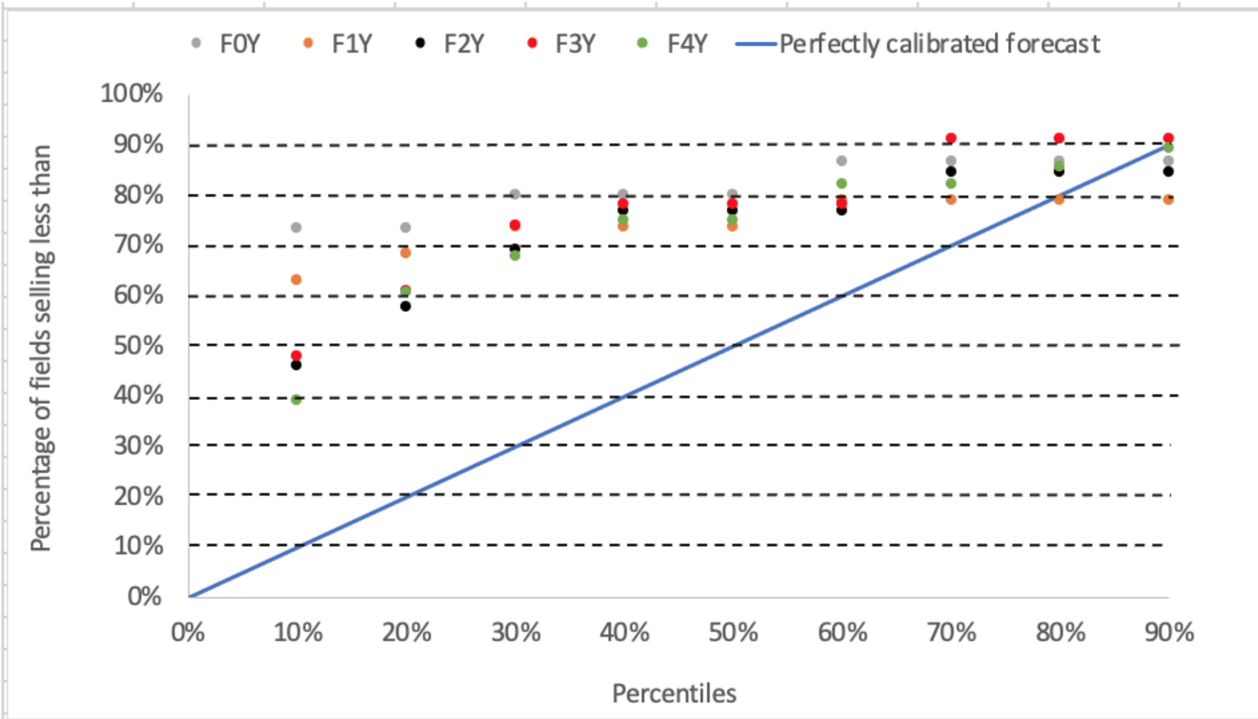

Fig. B.1.: Sensitivity analysis from F0Y to F4Y compared to actual sale start

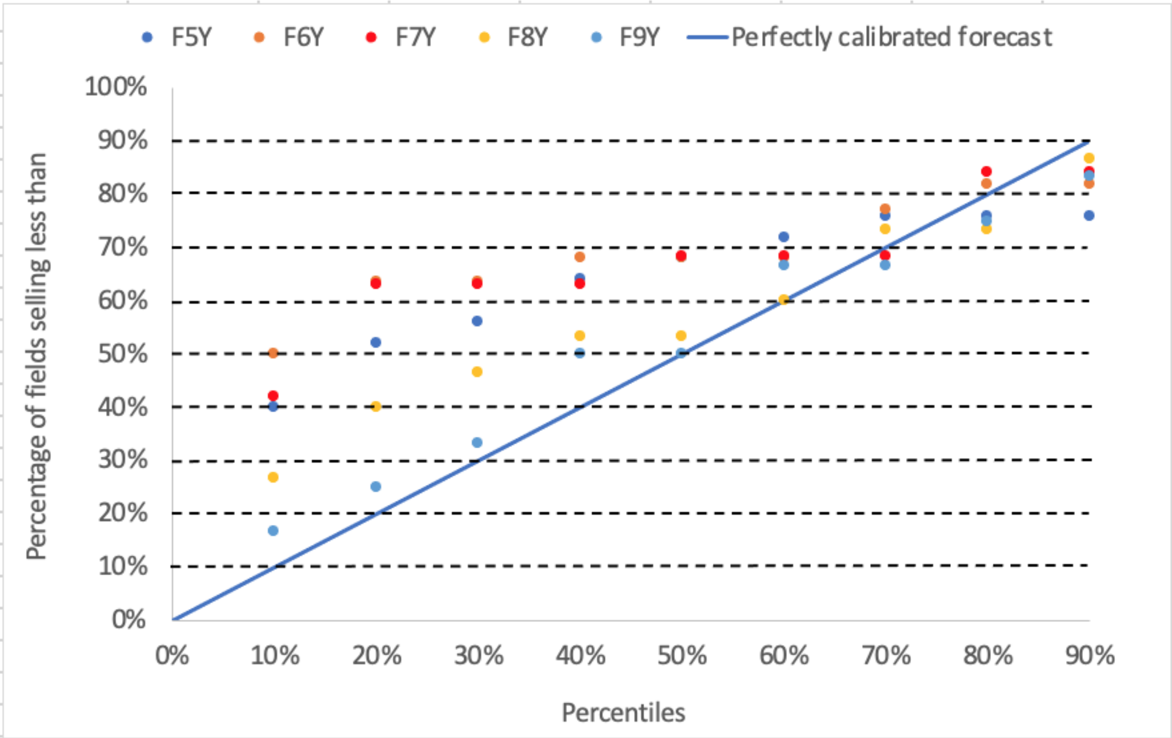

Fig. B.2.: Sensitivity analysis from F5Y to F9Y compared to actual sale start

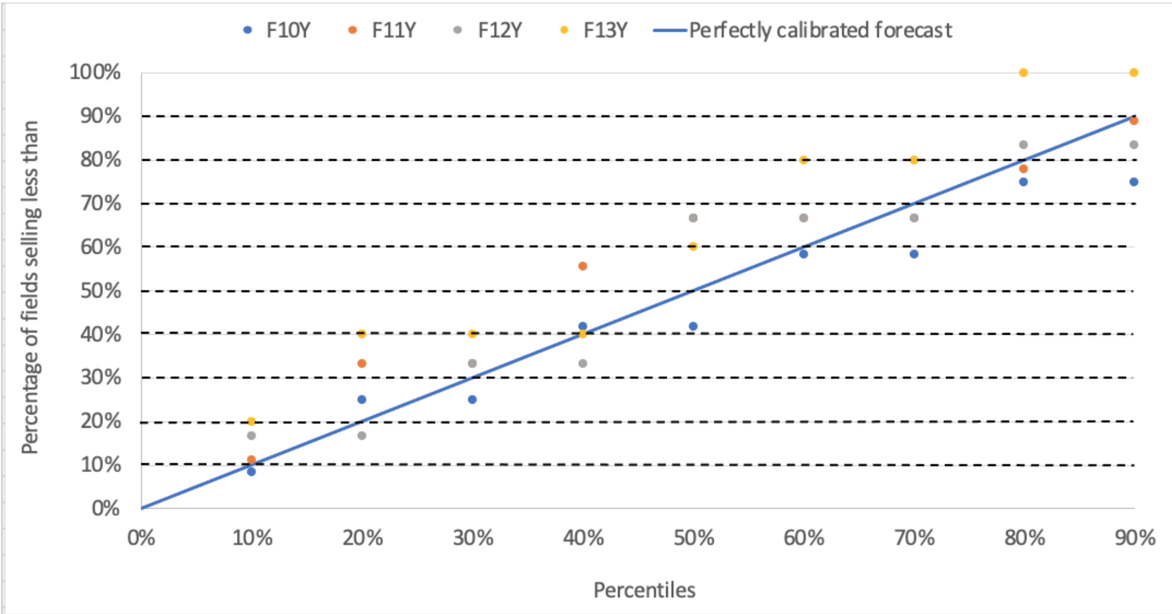

Fig. B.3.: Sensitivity analysis from F10Y to F13Y compared to actual sale start

C Number of fields when adjusting the relative mean error with all podp

Tab. C.1.: Overview of number of fields for different years when relative error is adjusted

	Number of fields																		
RE	F0Y	F1Y	F2Y	F3Y	F4Y	F5Y	F6Y	F7Y	FY8	F9Y	F10Y	F11Y	F12Y	F13Y	F14Y	F15Y	F16Y	F17Y	RODP
1%	13	15	21	21	23	23	19	15	13	10	10	9	6	5	3	2	1	1	210
2%	13	16	21	22	28	23	20	18	15	12	11	9	6	5	3	2	1	1	226
3%	13	17	21	22	28	24	21	18	15	12	11	9	6	5	3	2	1	1	229
4%	14	19	24	23	28	24	21	19	15	12	12	9	6	5	3	2	1	1	238
5%	15	19	26	23	28	25	22	19	15	12	12	9	6	5	3	2	1	1	243
6%	16	19	26	24	28	25	22	19	16	13	12	9	6	5	3	2	1	1	247
7%	18	20	26	24	30	25	22	19	16	13	12	9	6	5	3	2	1	1	252
8%	18	20	26	26	31	25	22	19	16	13	12	9	6	5	3	2	1	1	255
9%	19	21	26	26	31	25	22	19	17	13	12	9	6	5	3	2	1	1	258
10%	19	21	26	26	31	25	22	20	17	13	12	9	6	5	3	2	1	1	259
U	20	23	28	28	31	25	23	20	17	13	12	9	6	5	3	2	1	1	267

D Scatter plots; Without including the delay

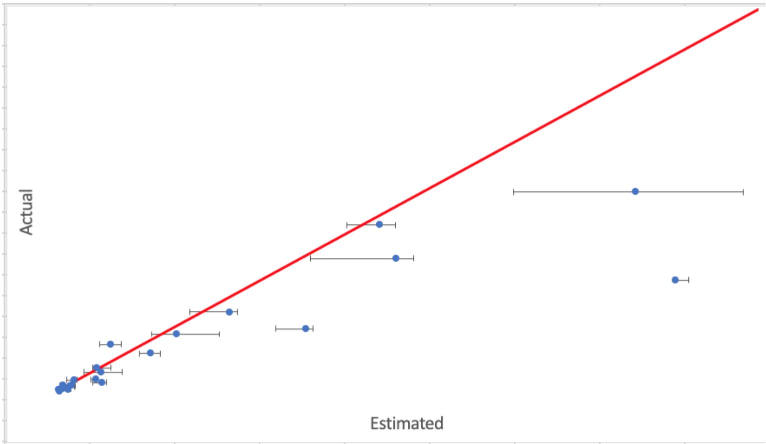

Fig. D.1.: Without delay: Scatter plot for all fields for F3Y

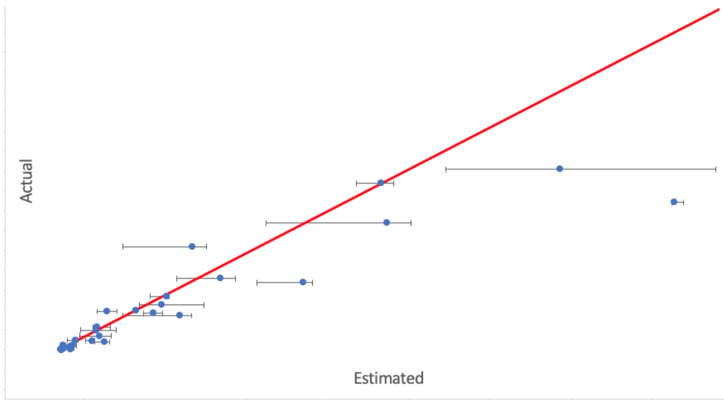

Fig. D.2.: Without delay: Scatter plot for all fields for F4Y

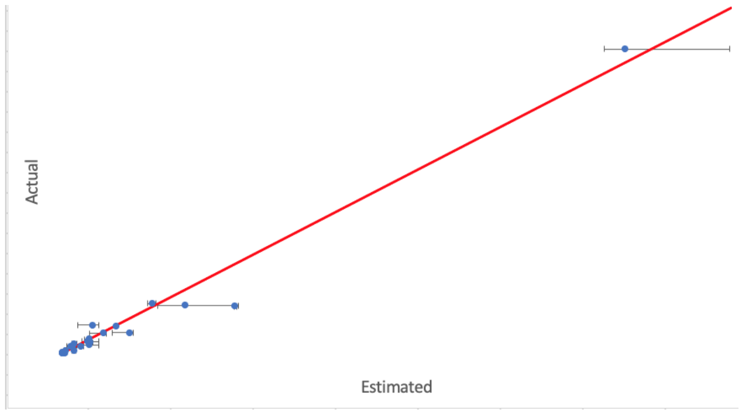

Fig. D.3.: Without delay: Scatter plot for all fields for F5Y

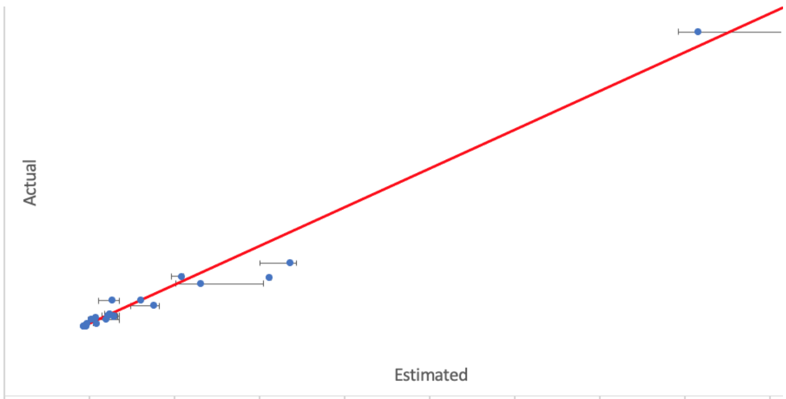

Fig. D.4.: Without delay: Scatter plot for all fields for F6Y

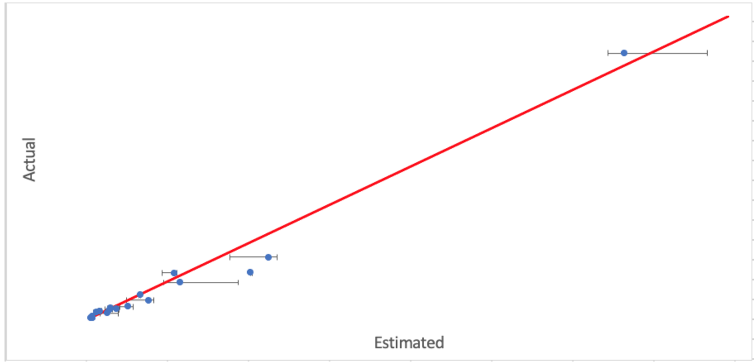

Fig. D.5.: Without delay: Scatter plot for all fields for F7Y

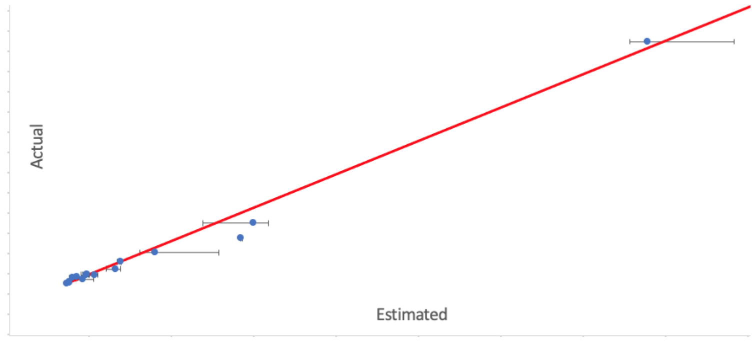

Fig. D.6.: Without delay: Scatter plot for all fields for F8Y

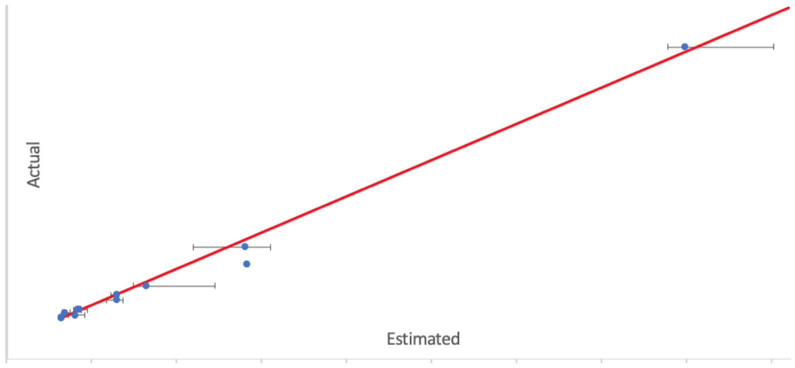

Fig. D.7.: Without delay: Scatter plot for all fields for F9Y

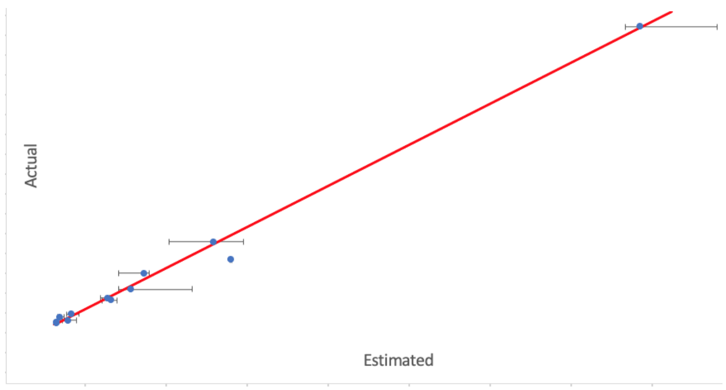

Fig. D.8.: Without delay: Scatter plot for all fields for F10Y

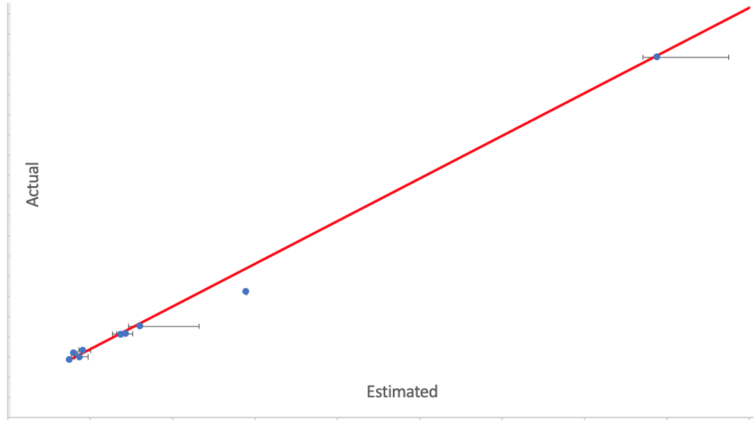

Fig. D.9.: Without delay: Scatter plot for all fields for F11Y

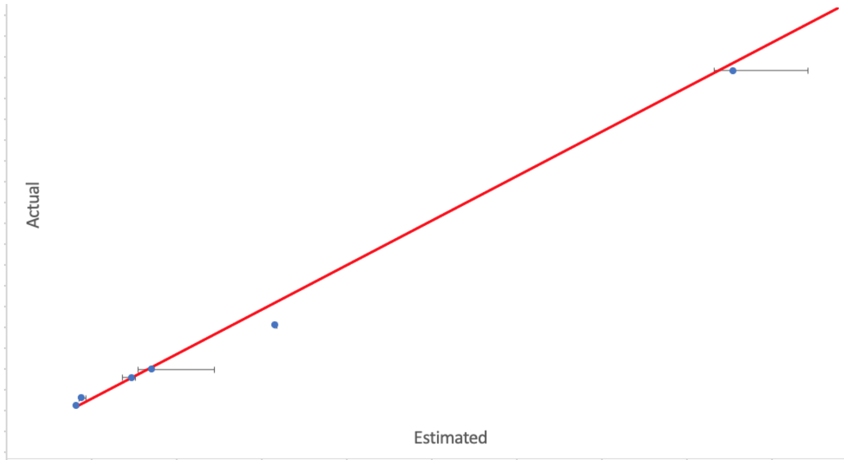

Fig. D.10.: Without delay: Scatter plot for all fields for F12Y

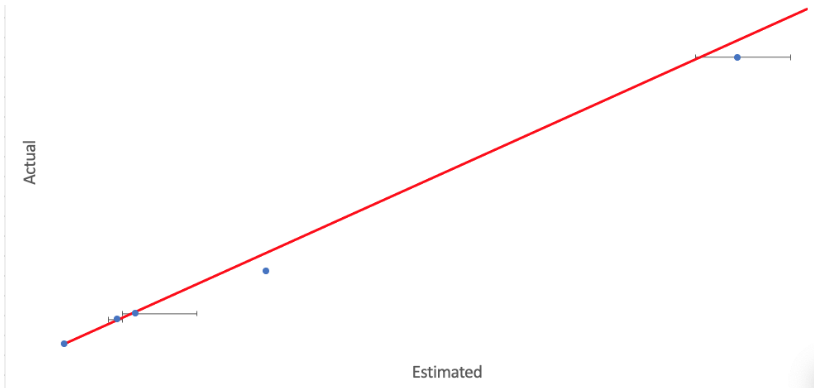

Fig. D.11.: Without delay: Scatter plot for all fields for F13Y

Scatter plots; Including the delay

E

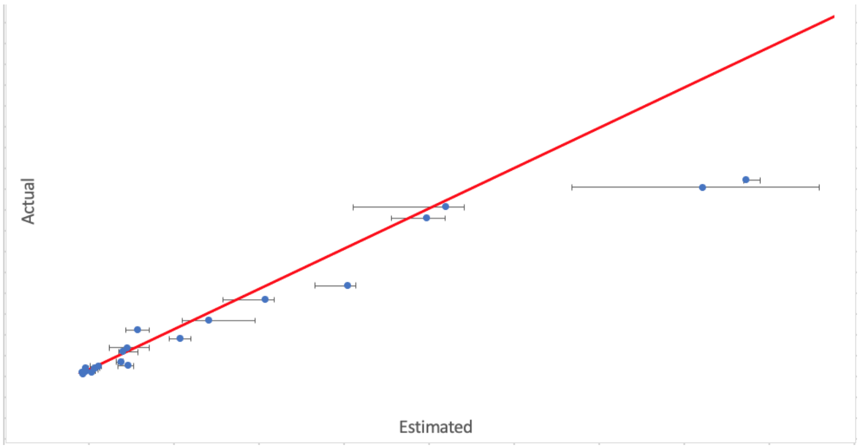

Fig. E.1.: With delay: Scatter plot for all fields for F3Y

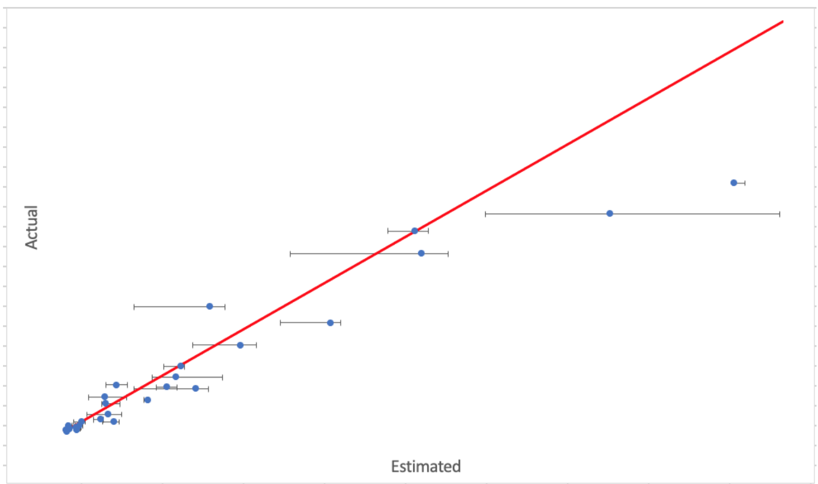

Fig. E.2.: With delay: Scatter plot for all fields for F4Y

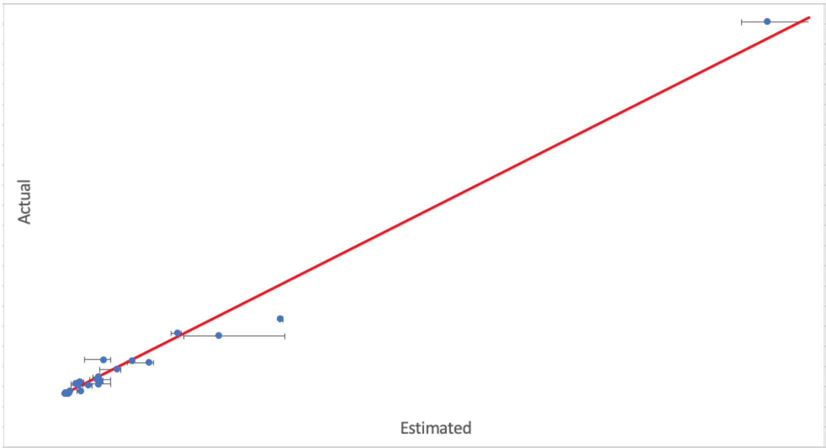

Fig. E.3.: With delay: Scatter plot for all fields for F5Y

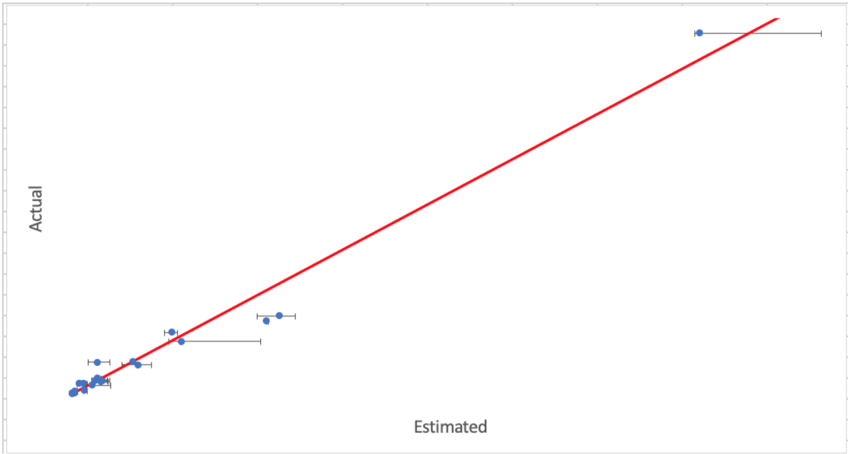

Fig. E.4.: With delay: Scatter plot for all fields for F6Y

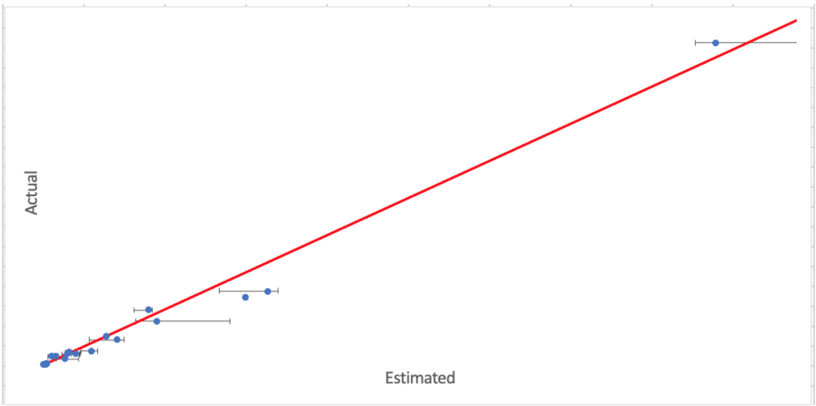

Fig. E.5.: With delay: Scatter plot for all fields for F7Y

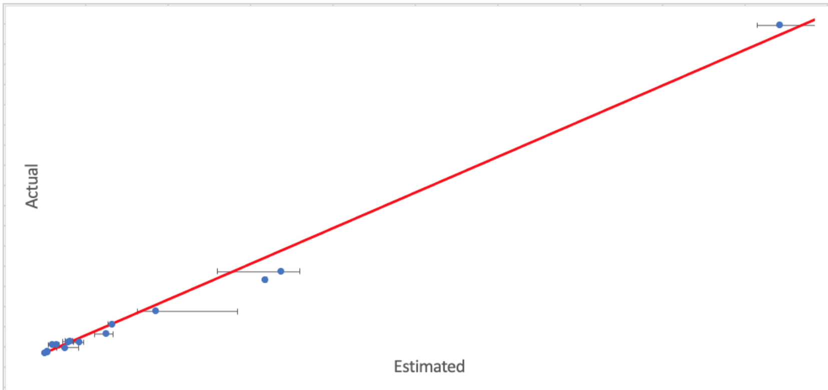

Fig. E.6.: With delay: Scatter plot for all fields for F8Y

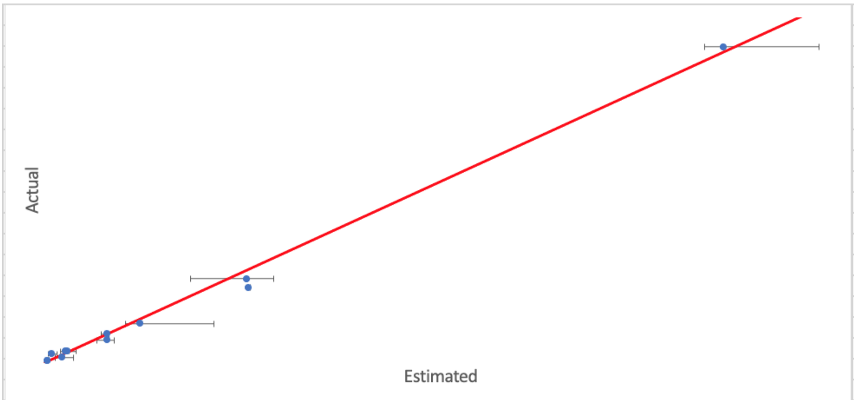

Fig. E.7.: With delay: Scatter plot for all fields for F9Y

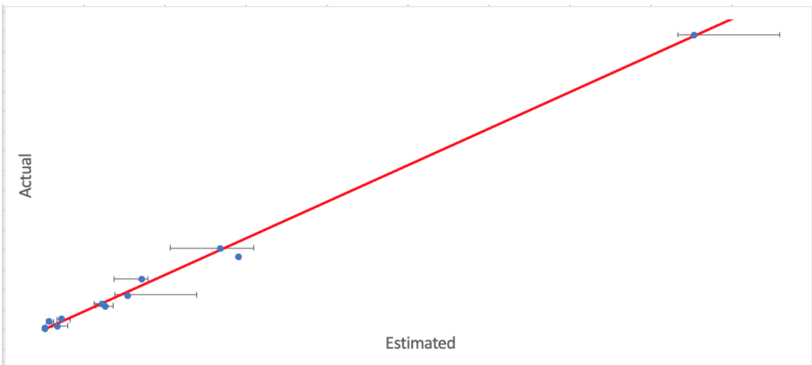

Fig. E.8.: With delay: Scatter plot for all fields for F10Y

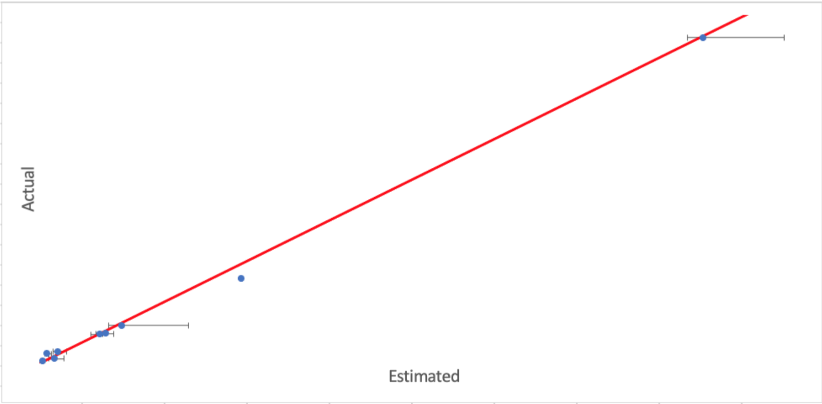

Fig. E.9.: With delay: Scatter plot for all fields for F11Y

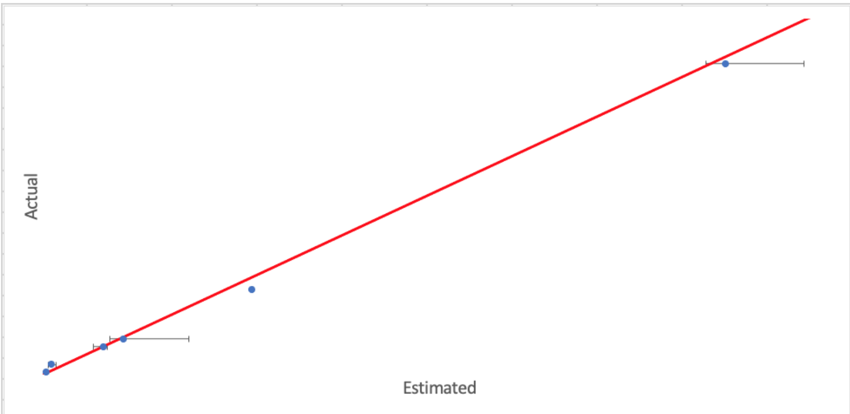

Fig. E.10.: With delay: Scatter plot for all fields for F12Y

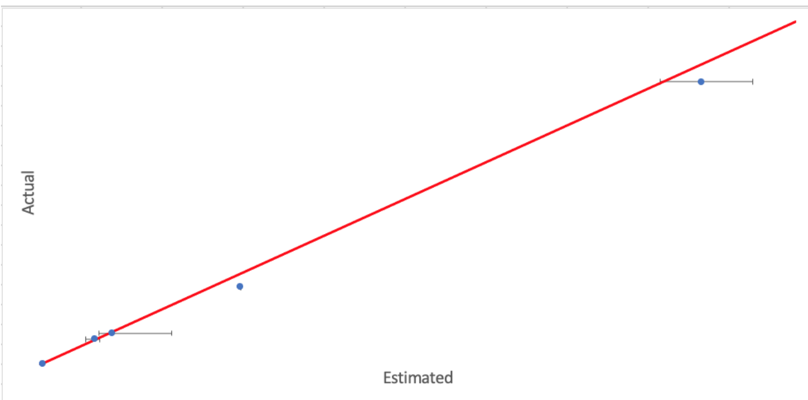

Fig. E.11.: With delay: Scatter plot for all fields for F13Y